Seismic Response of RC Members Subjected to the 2009 L'Aquila (Italy) Near-Field Earthquake Ground Motions

Report No. 10-01

Luigi Di Sarno
Amr S. Elnashai
Gaetano Manfredi

February 2010

ABSTRACT

The present work assesses the seismic response of reinforced concrete (RC) members subjected to horizontal (HGMs) and vertical (VGMs) ground motions recorded during the 2009 L'Aquila (Italy) earthquake. Normalized axial loads in beam-columns as well as the peak ground acceleration ratios between horizontal and vertical ground accelerations are emphasised as they are considered parameters of paramount importance for the assessment of structural components and systems subjected to combined horizontal and vertical ground motions (HVGMs).

Results of extensive parametric nonlinear dynamic analyses carried out on simplified structural models are discussed in detail. The sample models comprise cantilever RC columns and a two-storey, two-bay plane frame designed for gravity loads. The response quantities for the performed analyses are expressed in terms of axial loads, axial deformations, bending moment-axial load interaction and shear demand/capacity ratios. It is found that the variation of axial loads is significant in columns under HVGMs, especially in compression. For values of normalized axial loads (ν) corresponding to actual RC columns in framed building structures, e.g., normalized axial load ν>0.10, the average increase of the compression load ranges between 174% (ν=0.20) and 59% (ν=0.50). For high values of normalized axial loads the computed axial load-bending moment pairs lie beyond the threshold interaction curves and, in turn, the RC members fail. The shear demand-to-supply ratio is also detrimentally affected by the high fluctuations of axial loads in the columns. Net tensile forces were computed for columns with low-to-moderate axial gravity preload. In multi-storey framed buildings, the response of central columns is significantly affected by the HVGMs. Reliable seismic performance assessment of framed systems requires that combined HGMs and VGMs should be accounted for in the analyses.

LIST OF FIGURES

Figure 21 – Bending moment–axial load interaction (AQA record: East-West component): column preloaded with design normalized axial loads.

Figure 22 – Bending moment–axial load interaction (AQA-North-South component): actual normalized axial loads.

Figure 23 – Shear response (north-south component: AQA record): horizontal (*left*) and horizontal and vertical (*right*): design normalized axial loads.

Figure 24 – Base shear time history response (AQA-North-South component).

LIST OF TABLES

TABLE OF CONTENTS

INTRODUCTION

There is renewed interest in the assessment of near-field motions as it has been observed that the ratio of vertical-to-horizontal peak ground acceleration can be larger in near-fault than far-fault records (e.g. Bozorgnia and Campell, 2004; Elgamal and He, 2004; among many others). Moreover, there has been substantial field evidence worldwide demonstrating that numerous local and global collapses of structural systems employed for existing structures were caused by the devastating effects of the vertical component of earthquake ground motions (Broderick *et al*., 1994; Goltz, 1994; Elnashai *et al*., 1995; Youssef *et al*., 1995; Watanabe *et al*,, 1998; Naeim *et al*., 2000; FEMA 355E, 2000). In the wake of the recent 6 April 2009 L'Aquila (Abruzzo region, Italy) earthquake (M_w=6.3), several failure modes and collapses of reinforced concrete (RC) and masonry building structures, or non-structural components of the buildings especially those supported by cantilever systems, were attributed to the effects of the vertical seismic actions on structures. Figure 1 shows some examples of observed collapse of nonstructural components and secondary systems that may be caused by the vertical earthquake loading. Nevertheless, field evidence has not yet been supported by thorough analytical assessment and experimental tests.

Previous numerical studies on the evaluation of the effects of vertical ground motions (VGMs) in framed systems (Alaghebandian *et al*., 1998; Alaghebandian *et al*., 1999; Kunnath *et al*., 2008) have demonstrated that such motions may:

- Change the axial forces in columns;
- Increase bending moment and shear force demands in structural components and connections;
- Amplify plastic deformations;
- Extend plastic hinge formations;
- Reduce the available ductility of structural components and connections.

The above response characteristics were also derived during recent experimental tests carried out on RC circular columns (Kim and Elnashai, 2008). The outcomes of the performed tests showed that VGMs do not affect significantly the storey shear and lateral drift. Conversely, the vertical component of ground motions may generate high fluctuations of axial loads in the columns and, in turn, endanger the shear capacity. The occurrence of concrete crushing caused the collapse of many RC columns. The onset of likely high compression forces induced by VGMs are thus detrimental for the seismic response of RC beam-columns. Such response depends, however, on the level of axial preload in the member. For example, in multi-storey framed buildings, axial forces in the upper storey columns rather than in the lower columns are considerably affected by VGMs. In

first storeys of buildings, the vertical component of the simultaneous ground motions has negligible effects on the axial forces of the exterior columns because of earthquake-induced overturning.

Figure 1 – Collapse of non-structural components in residential reinforced concrete (RC) multi-storey framed buildings in the outskirt of L'Aquila during the 6 April 2009 (Italy) earthquake, designed according to allowable-stress (*top*), limit state (*bottom*) seismic codes .

The above numerical and experimental studies considered primarily framed systems behaviour and did not adequately account for variation of the axial preload on the seismic response of beam-columns.

The present study provides insight into the seismic response of RC members subjected to horizontal (HGMs) and vertical (VGMs) earthquake ground motions. The normalized axial loads in beam-columns, as well as the peak ground acceleration (PGA) ratios between horizontal and vertical ground accelerations, are emphasised as they are considered parameters of paramount importance for the assessment of structural components and systems subjected to both HGMs and VGMs.

Results of comprehensive parametric nonlinear dynamic analyses carried out on simplified structural models are presented and discussed hereafter in detail. Plane (2D) systems are employed for the seismic assessment as they are considered reliable models for the target of the performed

analyses. The structural performance is assessed with respect to global response parameters; local effects, such as, for example, bond-slip mechanisms, are deliberately not accounted for.

EARTHQUAKE INPUT CHARACTERIZATION

The 6 April 2009 L'Aquila (Italy) earthquake was generated by a normal fault with north-west/south-east trend; the dip of the fault is along the South-West direction. The main shock occurred at 01:32:39 GMT with a magnitude M_w=6.3 close to the town of L'Aquila (located at about 6 km northeast to the epicenter). In this analytical study, four natural near field records (distance from the fault less than 10km) from the 2009 L'Aquila earthquake were selected for the response-history analyses: Aterno River (AQA), Grilli Hill (AQG), Aquila Eng. Park (AQK) and Central Valley (AQV). They are a subset of the 168 strong motions of the 6 April 2009 L'Aquila earthquake, which were recorded by 56 stations of the national network, Rete Accelerometrica Nazionale (RAN); these stations are located at a distance from the earthquake fault varying between 4.3 km (L'Aquila-Aterno Valley, Grilli Hill) and 279.4 km (Genzano di Lucania). The acceleration time histories employed in this study are also available on the official website of the National Civil Protection (www.protezionecivile.it); the waveforms were corrected with the linear baseline and filtered using the Butterworth bandpass (Hp = 0.1 Hz and Lp = 50Hz); further details on such waveforms can also be found in Chioccarelli *et al*. (2009), among many others.

The PGA and the ratio between the vertical $(PGA)_v$ and horizontal $(PGA)_h$ for the sample records are summarised in Table 1, in which the ratios were computed for both longitudinal and transverse (horizontal) components of the strong motions. The soil type for the AQ-stations varies between B and C according to the classification implemented in CEN (2006-b) and Ministero delle Infrastrutture (2008); further details on the AQ-stations can be found in several earthquake reconnaissance reports (e.g., Pacor and Paolucci, 2009, among many others).

		Coordinates		PGA (g)			Vertical / Horizontal Ratio $(PGA)_v$ / $(PGA)_h$	
Station	Label	Latitude	Longitude	North-South	East-West	Up-Down	North-South	East-West
ATERNO RIVER	AQA	42.37553	13.3393	0.444	0.404	0.470	1.058	1.164
GRILLI HILL	AQG	42.37347	13.33703	0.517	0.475	0.243	0.471	0.512
AQUILA ENG: PARK	AQK	42.34497	13.40095	0.354	0.334	0.372	1.052	1.116
CENTRAL VALLEY	AQV	42.37722	13.34389	0.546	0.659	0.522	0.957	0.793

Table 1 – Station location and ratio of the vertical-to-horizontal peak ground accelerations (PGA) in the 6 April 2009 L'Aquila (Italy) earthquake.
Note: All the stations are located in L'Aquila – Aterno Valley.

It is noted that the $(PGA)_h$ ranges between 0.334g (AQK) and 0.659g (AQV). The values of the $(PGA)_v$ vary between 0.243g (AQG) and 0.522g (AQV). The ratios of the vertical-to-horizontal accelerations are high; for two stations (namely AQA and AQK), the PGAs of the vertical

component exceed the values of the horizontal counterparts. The time histories of the three components (North-South, East-West and Up-Down) of the ground motions recorded at AQA, AQG, AQK and AQV were employed to perform the response history analyses that follow. The ratio of the vertical-to-horizontal peak accelerations is shown in Figure 2 as a function of the epicentral distance, and for RAN stations up to 150 km from the seismic source. It is noted that the vertical component tends to exceed the horizontal one up to an epicentral distance of about 30 km. The computed values do not comply with the 2/3 rule proposed by Newmark and Hall (1982); this finding confirms that the rule does not apply to near-field earthquakes, as reported in the literature (e.g. Elnashai and Papazoglou, 1997; Bozorgnia and Campell, 2004; Elgamal and He, 2004). The vertical-to-horizontal (V/H) peak attenuation by Elnashai and Papazoglou (1997) is also included in Figure 2. It is noted that the scatter between the recorded motions and the predicted values is high; the V/H ratios are in the range predicted by the attenuation relationships corresponding to earthquakes with M_S=6.5 and M_S=7.5; the latter values are higher than that estimated for the 6 April 2009 L'Aquila earthquake.

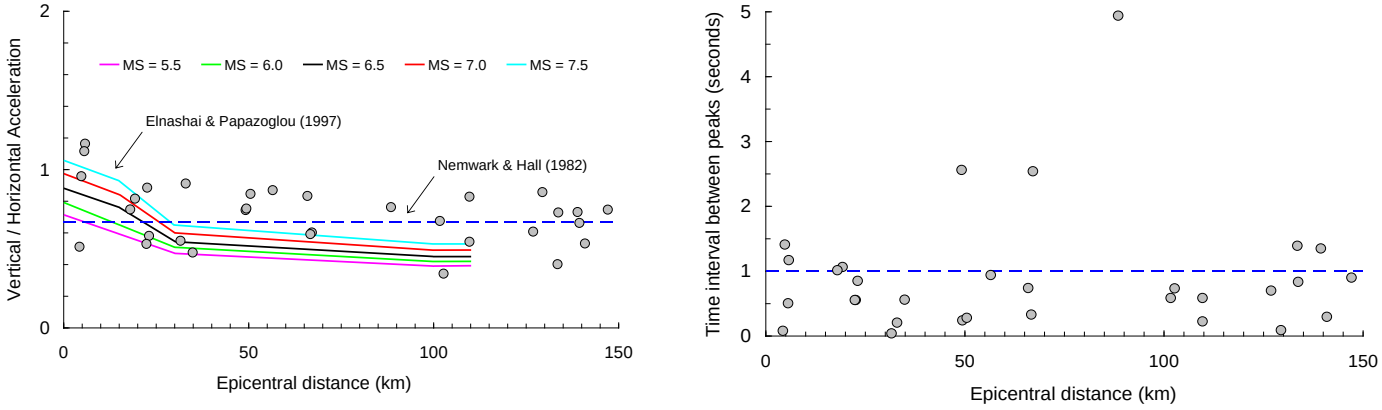

Figure 2 – Vertical/horizontal acceleration ratios as a function of the epicentral distance for the recording stations (up to 150 km away from the fault) (*left*) and time interval between peaks (*right*) for the recording stations (up to 150 km away from the fault) of the 6 April L'Aquila earthquake. The dotted line corresponds to the 2/3 ratio proposed by Newmark and Hall (1982).

The time intervals (or time delay) between the acceleration peaks of the horizontal and vertical components provided in Figure 2 show that the delay between the onset of the peaks are small, particularly for AQ-stations: the delay is 0.11 seconds for AQG and 0.84 seconds for AQK. The distribution of the time interval between horizontal and vertical ground motions indicates that the time delay between peaks varies with source distance but it is generally within 5 seconds. For the sample records the delay is rather small because the recording stations are less than 5 km away from the fault rupture.

The simultaneous occurrence of the peaks in the acceleration time history may have devastating structural effects; however, a recent study by Kim and Elnashai (2008) has

demonstrated that the damage pattern and failure modes of structures are affected significantly by the ratios of the vertical-to-horizontal peaks of the acceleration time history and they are not significantly dependent on the time delays.

Elastic spectral acceleration, velocity and displacement response of the AQA, AQG, AQK and AQV earthquake records were also evaluated. The results are summarised in Figure 3. Near-source long-period pulses, possibly related to source effects, i.e. forward-directivity and fling-step phenomena (Somerville, 2000), are present in all the records. However, the effect of the site response is visible in the AQK record, which shows the highest long period content, and in the AQA record, which exhibits a low-period content.

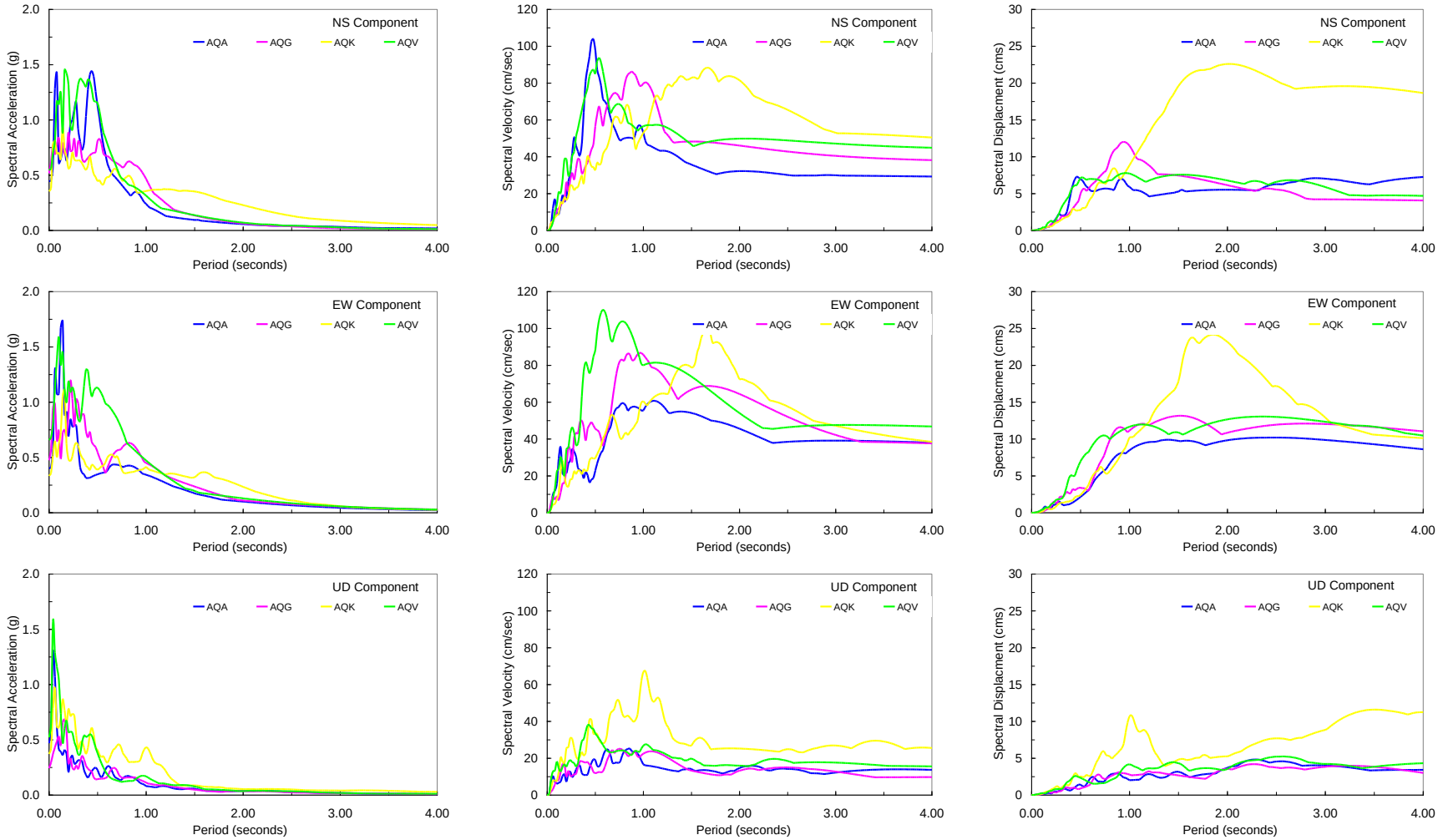

Figure 3 – Acceleration (*left*), velocity (*middle*) and displacement *(right*) response spectra of the recorded earthquake ground motions: north-south (*top*), east-west (*middle*) and vertical (*bottom*) components.

Elastic acceleration response spectra of the recorded ground motions (horizontal and vertical components) were also computed and compared to the new Italian code spectra (Ministero delle Infrastrutture, 2008) for ordinary buildings (i.e. with return period T_R = 975yrs) and critical facilities (i.e. with return period T_R = 2475yrs). The results are provided in Figure 4. The code spectra were computed for soil type C, according to the classification in Ministero delle Infrastrutture (2008), which is similar to that in CEN (2006-b); a 5% viscous damping was assumed.

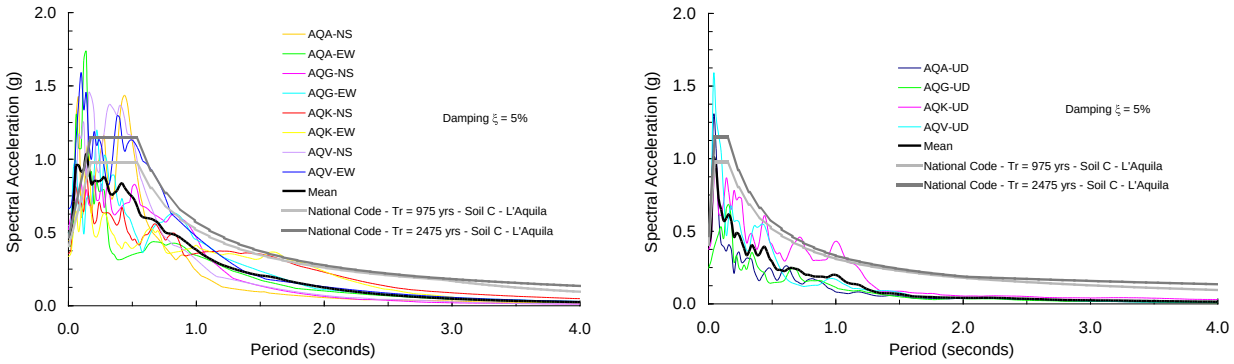

Figure 4 – Elastic acceleration response spectra of the recorded earthquake ground motions and national code spectra (Ministero delle Infrastrutture, 2008) for ordinary buildings (T_R = 975yrs) and critical facilities (T_R = 2475yrs): horizontal (*left*) and vertical (*right*) component.

The response spectra plotted in Figure 4 shows that both the horizontal and vertical components tend to exceed, especially for periods less than 1.0 second, the code-defined spectral values; however, the mean spectra are a closer match to the smooth spectra in the design standards. The values of the recorded peak ground accelerations and those implemented in the recent Italian seismic code (Ministero delle Infrastrutture, 2008) are compared in Figure 5 for both horizontal and vertical components of the earthquake.

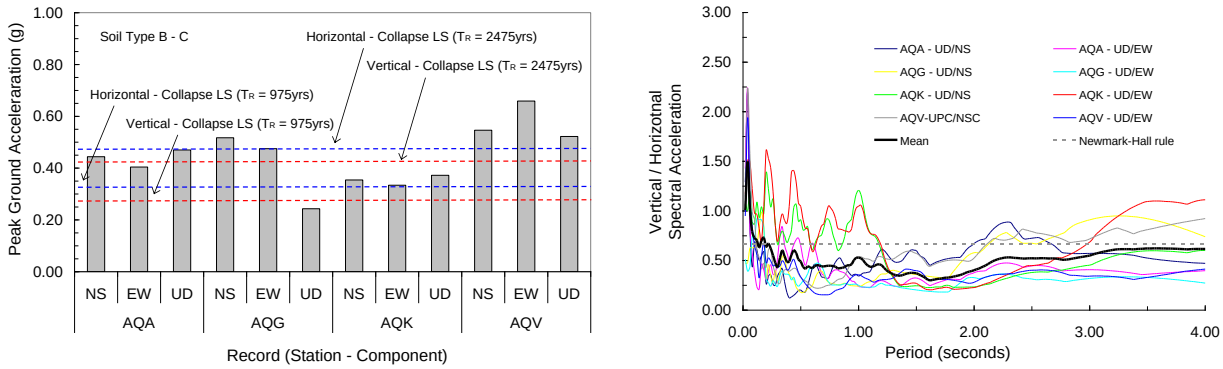

Figure 5 - Recorded peak ground accelerations and seismic code design accelerations (*left*) and ratio between the vertical and horizontal spectra (*right*).

The ratio of the spectral vertical-to-horizontal accelerations is shown in Figure 5 and shows that such ratio is particularly high for low periods of vibrations. The 2/3 rule by Newmark and Hall (1982) is also included in the plot of the spectral ratios in Figure 5; its use underestimates

considerably the spectral ordinates particularly at low periods. High spectral acceleration amplifications are observed for low periods of vibration, e.g., less than 0.5 seconds for the horizontal components of all sample records. This finding is further confirmed by the Fast Fourier Transforms (FFTs) of the waveforms. Predominant and mean periods of the records were also computed and are depicted in Figure 6.

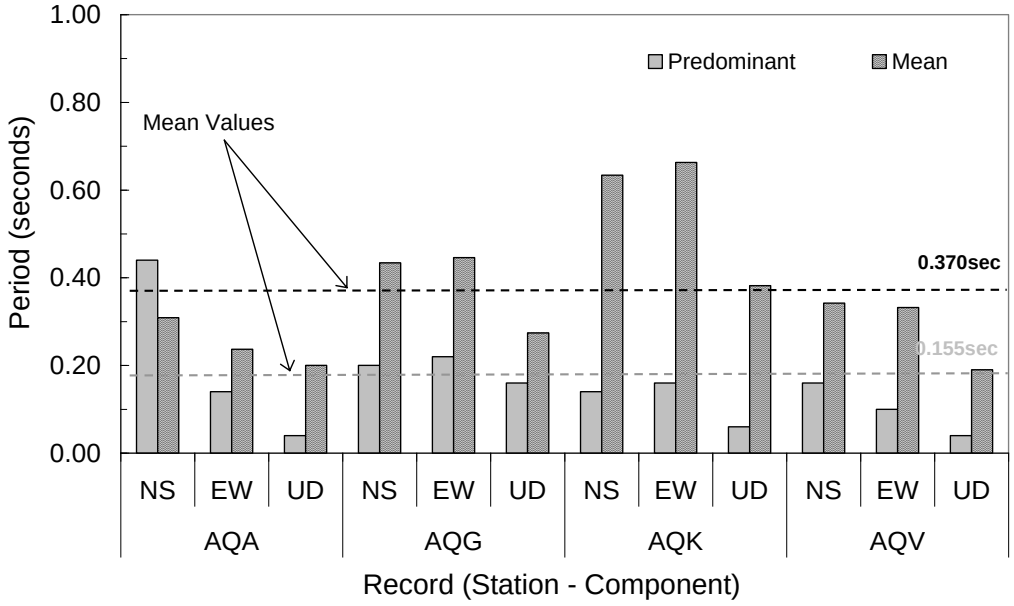

Figure 6 - Predominant and mean periods of the recorded earthquake ground motions.

The average time of the estimated predominant and mean periods is 0.155 seconds and 0.370 seconds, respectively. The observed high amplifications at low periods may affect detrimentally the response of stiff structural systems, e.g., low-rise RC framed buildings and chiefly masonry structures. The above periods of vibration, especially those relative to the vertical components of the earthquake ground motion, are close to the fundamental axial period of structural members.

SAMPLE MODELS

Two simplified models were considered in the following parametric study: a sample RC cantilever column (1.80m high) and a plane two-storey two-bay frame as shown pictorially in Figure 7. The cross-section of the cantilever column is assumed to be 30cm x 30cm; 4 smooth bars with ϕ =14mm and located at the section corners were utilized; the concrete cover is 2.5cm. The concrete strength is assumed to be 19MPa and the yield stress is equal to 330 MPa. The above properties correspond to typical columns of existing RC low-rise framed buildings (2 to 3 storeys) designed for gravity loads in the Mediterranean area.

The seismic assessment of the cantilever column was carried out with reference to six values of normalized axial load ($\nu = N_{Sd} / N_{pl.RD}$): the ν-factors vary between 0.05 (low level of axial load) and 0.50 (high level of axial load). Note that the values of the normalized axial loads were estimated with reference to the actual mechanical properties of the materials used for the sample column, i.e., the material partial safety factors for both steel and concrete (denoted γ_c and γ_s in the Eurocode 2 and Eurocode 8) are $\gamma_c=\gamma_s=1.0$. The coefficient for long term effects is $\alpha_c=1.0$. The (actual) squash load is $N'_{pl.RD}$ = 1913.28 kN. If the design value of the squash load is determined in compliance with CEN (2006-a), the value is $N_{pl.RD}$ = 1145.77kN. Table 2 summarises the normalized axial loads for sample RC columns.

The parametric response history analyses were carried out with reference to the design and actual values of the normalized axial loads.

The plane frame consists of a two-storey two-bay frame. The storey height are 3.75m (ground floor) and 3.60m (top floor); the clear span length is 2.55m. The cross sections of the columns are 30x30cm. Deep beams, with a cross-section 30x50cm, are placed on both the lower and top floor. The plane employs a RC solid slab; the thickness of which is 25cm at the ground floor and 20cm at the roof level. The layout of the frame and the relevant longitudinal and transverse reinforcements are displayed in Figure 7. The solid slab is used to simulate typical floor systems of framed buildings designed for gravity loads only and live loads of 3.0 kN/mq. The total uniform loads (dead and live) on the beams at the first and second floors are 16.56 kN/m and 14.0 kN/m, respectively. Smooth bars were used for the longitudinal and transverse steel reinforcement of beams and columns of the sample RC frame; the details of such reinforcement are shown in Figure 7.

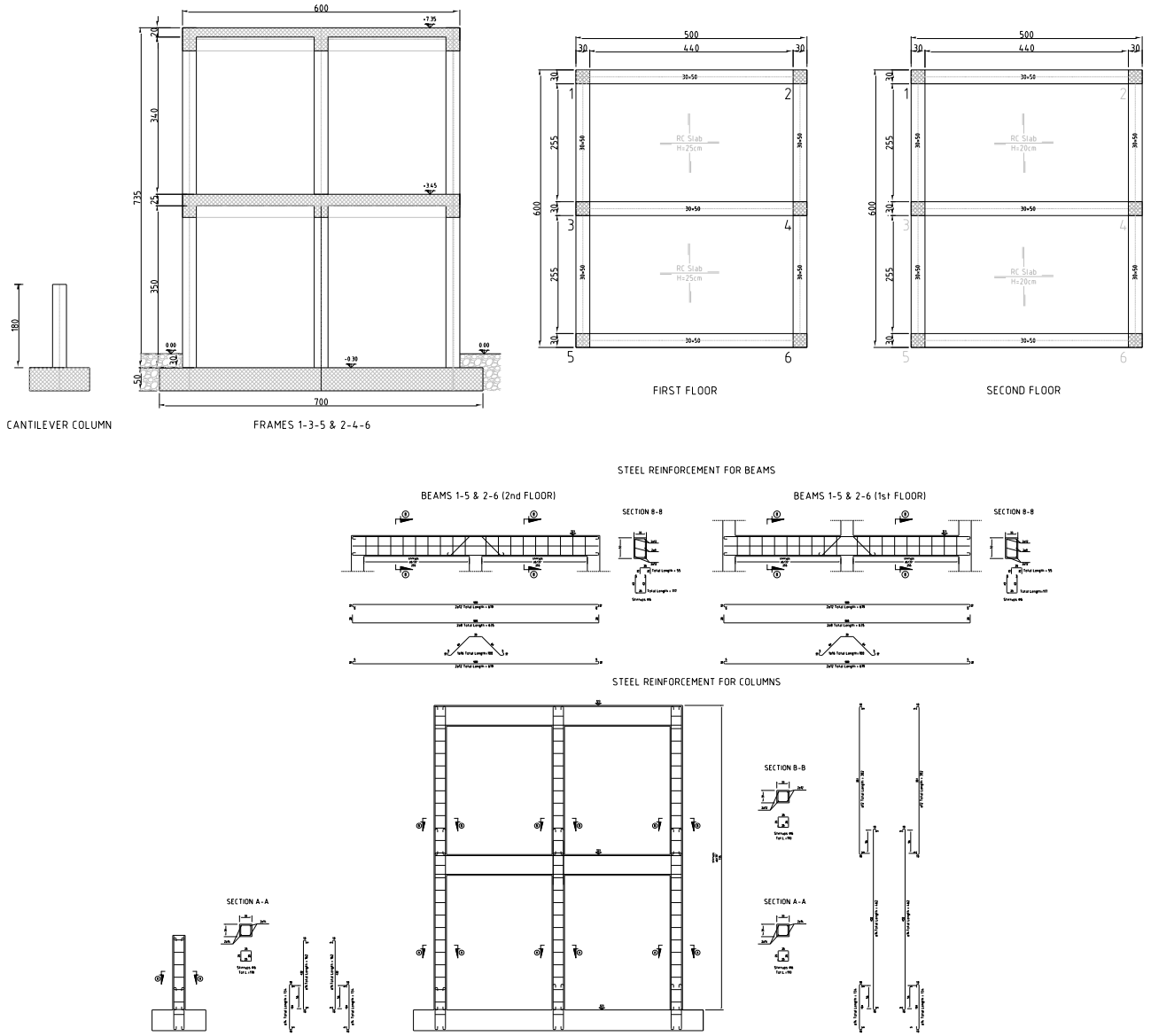

Figure 7 - Sample RC models employed for the inelastic analyses: geometry (*top*) and details of the steel reinforcement (*bottom*).

Bars with ϕ =14mm and located at the section corners were utilized for the columns; for the beams, longitudinal bars employ ϕ =8mm, ϕ =12mm and ϕ =16mm. The transverse reinforcement consists of rectangular stirrups with ϕ =6mm for both beams and columns. The concrete cover is 2.5cm. The concrete strength is assumed to be 19MPa and the yield stress is equal to 330 MPa. The columns of the frame have properties similar to those of the sample cantilever column.

NUMERICAL MODELLING

The finite element model (FEM) employed to discretize the cantilever column is restrained for out-plane displacements. A 35 tons-lumped mass is located at the top of the column; the lumped mass has only longitudinal, transverse and vertical translation degrees of freedom. Rotational masses are null. The axial loads are applied as concentrated loads at the column top.

The two-storey two-bay RC frame was modelled as a plane system. The masses are lumped at the beam-to-column intersections. The values of the computed masses are 2.41 tons and 4.81 tons for the first floor, while 4.07 tons and 2.04 tons were utilized for the roof. Dead and live loads are applied as point loads along the beams of the first and top floors.

The finite element program used to perform the response history analyses is Zeus-NL (Elnashai *et al*., 2004). This program is capable of predicting the large displacement response of spatial frames under static or dynamic loading, taking into account both geometric nonlinearities and material inelasticity. The spread of inelasticity along the member length and across the section depth is explicitly modelled, allowing for accurate estimation of damage distribution. The interaction between axial force and transverse deformation of the frame element (beam-column effect) is implicitly incorporated in the element cubic formulation implemented in the computer program, whereby the strain states within the element are completely defined by the generalized axial strain and curvature along the element reference axis (x), while a cubic shape function is employed to calculate the transverse displacement as a function of the end-rotations of the element. To evaluate accurately the structural damage distribution, the spread of material inelasticity along the member length and across the section area is explicitly represented through the employment of a fibre modelling approach, as shown in Figure 8. The sectional stress-strain state of beam-column elements is obtained through the integration of the nonlinear uniaxial

stress-strain response of the individual fibres in which the section is subdivided. The discretization of a typical RC cross-section of the structural members of the sample models is also displayed in Figure 8.

The distribution of material nonlinearity across the section area is accurately modelled, even in the highly inelastic range, due to the selection of 200 fibres employed in the response history analysis of the sample beam-column. A 2D finite element model was employed, which may be considered sufficiently accurate and reliable for the purpose of the present numerical study. The beam-column is discretized using 6 nonlinear cubic elements; the mesh includes smaller elements concentrated at the member edges (Figure 8). The length of the two edge elements is 10% of the element clear span; the central elements are 30% of the total member length. Thus, the spread of inelasticity along member length is accurately estimated. Two integration Gauss points per element are used for the numerical integration of the governing equations of the cubic formulation (stress/strain results in the adopted structural model refer to these Gauss Sections, not to the element end-nodes). Consequently, at least two Gauss points are located in the inelastic region at the base of the column in order to investigate adequately the spreading of plasticity in the critical region and within the structural member. At least two Gauss points are also placed in the critical regions of beams and columns in the plane frame, as also schematically illustrated in Figure 8.

A bilinear model with kinematic strain-hardening was utilized to simulate the inelastic response of steel longitudinal bars of the cross-sections of the RC beam-column. A strain hardening equal to 0.015 (or 1.5%) was assumed for the post-yield response. The modulus of elasticity E is 2.0 E+05 MPa. The concrete was modelled through a nonlinear constant confinement model. This is a uniaxial nonlinear model initially implemented by Madas and Elnashai (1992) that follows the constitutive relationships formulated by Mander *et al*. (1988) and the cyclic rule proposed by Martinez-Rueda and Elnashai (1997). The confinement effects provided by the lateral transverse reinforcement are incorporated through the rules suggested by Mander *et al*. (1988) whereby constant confinement pressure is assumed throughout the entire stress-strain range. The model calibrating parameters utilized to fully describe the mechanical characteristics of the material include (i) compressive strength, (ii) tensile strength, (iii) strain at peak stress and (iv) confinement factor. For the sample beam-column, values of the confinement factor k were assumed equal to 1.1 and 1.0 for confined (core) and unconfined (shell) concrete,

respectively. A value of 19MPa was adopted to simulate the compressive strength of concrete; the tensile strength is 1.9MPa. The strain at peak stress is 0.002; collapse strains are 0.005 and 0.003 for confined and unconfined concrete, respectively. Such strain values were determined on the basis of typical actual response of RC beam-columns designed primarily for gravity loads, i.e. low ductility members.

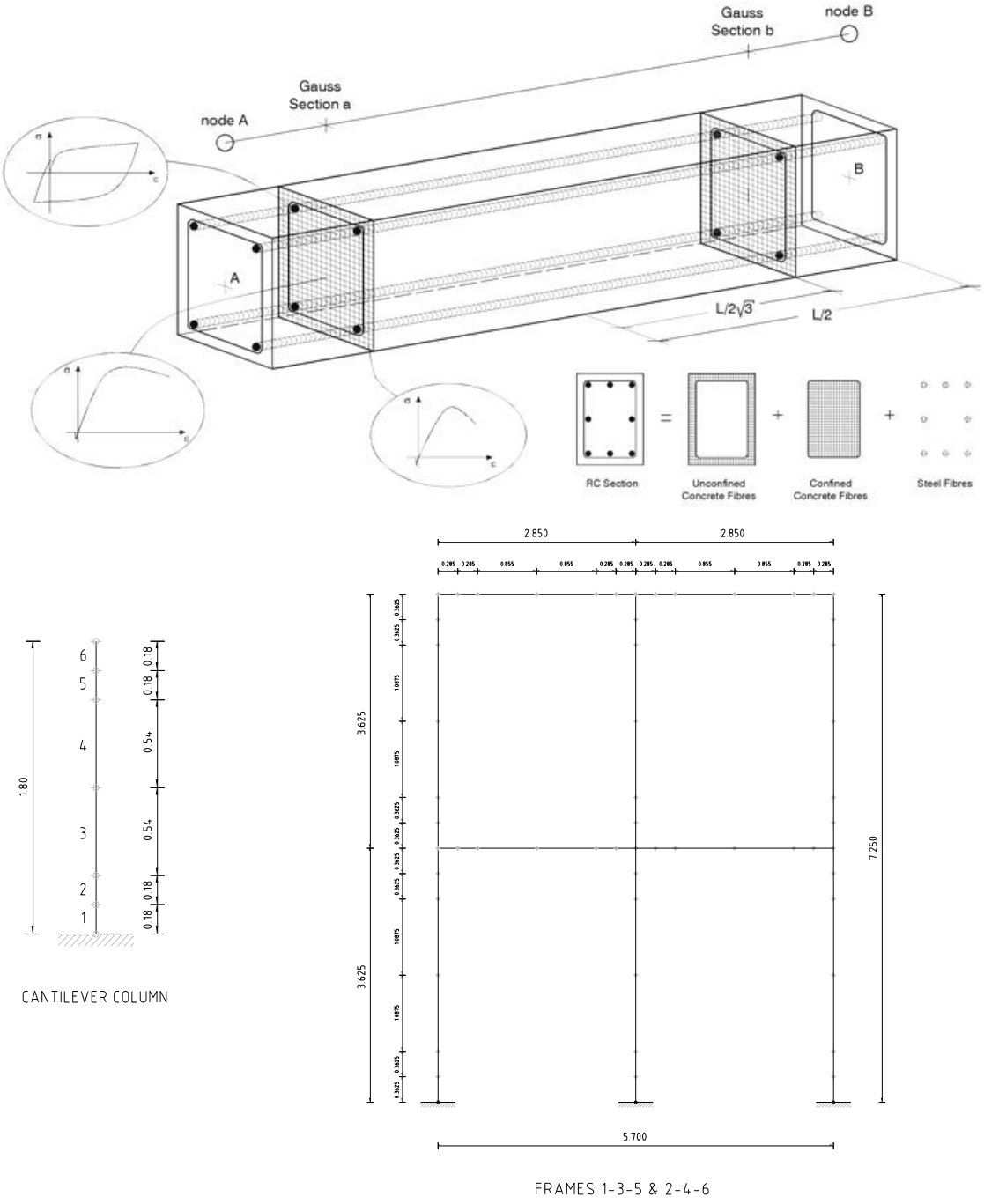

Figure 8 – Fibre discretization of the frame element in the analytical model.

It is instructive to mention that local effects, such as bond-slip effects, are not implemented in the sample finite element models; the target of the performed parameter analyses is to investigate the global response of RC beam-columns subjected to combined horizontal and vertical components of earthquake ground motions. Furthermore, it is assumed that the sample RC members are in the uncracked stage at the beginning of the earthquake loading. The above assumption can be realistically accepted for the typical RC buildings located in Italy. Additionally, the emphasis of the present study in on the ultimate structural response of RC beam-columns. The significant stiffening effect of the infills was not considered in the study. The effect of the presence of the masonry infills is currently under investigation

MODAL RESPONSE

Eigenvalue analysis was carried out for the cantilever RC column and the plane frame to determine the modal properties of the structural systems. In so doing, the detailed FEMs employing the discretization illustrated earlier were utilized. The presence of longitudinal reinforcement bars within the section was accounted for through the use of fibre-based modelling. The periods of vibration of the sample models were determined using the Lanczos algorithm implemented in Zeus-NL (Elnashai *et al*., 2004).

The sample RC column has a natural period equal to 0.414 seconds for horizontal oscillations; the vertical period of vibration is 0.036 seconds. The latter period was also verified by utilizing scaled natural records (scaling factor 1/10, maximum acceleration lower than 0.06g) corresponding to AQA, AQG, AQK and AQV. To estimate the axial period of the column, the dynamic axial load records were used. The top acceleration response history was assessed with the Fast Fourier Transform (FFT) analysis. The results are shown in Figure 9, where the spike corresponds to a resonance in the response and indicates the fundamental period of vibration along the vertical axis of the beam-column. The computed axial period is 0.038 seconds thus matching the value computed with the modal analysis, i.e., 0.036 seconds. The above value was also derived by means of the response spectrum (Figure 9); the assumed viscous damping is 1%. The latter value, which is lower than the 5% viscous damping typically utilized for horizontal vibrations of RC structures, accounts for the reduced inelasticity associated to the vertical oscillations.

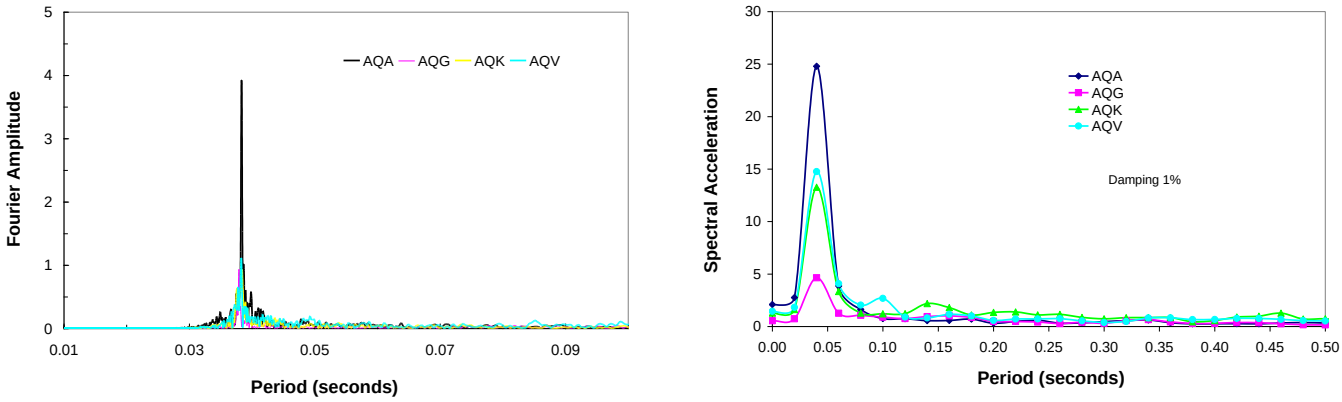

Figure 9 - Fast Fourier Transform of the acceleration at the top of the column (*left*) and response spectrum of the acceleration response history at the top of the column (*right*)

Modal analysis carried out for the plane frame showed that the periods of vibration are 0.296 seconds (first mode with an effective modal mass percentage equal to 93.28%) and 0.112 seconds (second mode and an effective modal mass percentage of 6.72%); the vertical period is 0.027 seconds. The computed periods are similar to those relative to the several existing RC framed buildings located in the Southern European regions (e.g. Gallipoli *et al*., 2009; Masi and Vona, 2009, among others).

SEISMIC RESPONSE ASSESSMENT

The sample RC column and the two-storey two-bay plane frame was subjected to horizontal and combined horizontal and vertical components (HVGMs) of earthquake ground motions; the structural assessment was carried out by means of nonlinear time history analyses. A total number of about 200 (124x4=192) inelastic analyses were carried out using the sample RC cantilever columns; 12 levels of axial loads (6 values for the design and 6 values for the actual normalized squash load) were considered as outlined in Table 2. The North-South and East-West components relative to AQA, AQG, AQK and AQV recording stations were employed as horizontal components of the earthquake ground motions (HGM); combined HVGMs were also considered.

Squash Load	$\nu = 0.05$	$\nu = 0.10$	$\nu = 0.20$	$\nu = 0.30$	$\nu = 0.40$	$\nu = 0.50$
Design Value (kN)	57.29	114.58	229.16	343.74	458.32	572.90
Actual Value (kN)	95.66	191.32	382.64	573.96	765.28	956.60

Table 2 – Normalized axial loads estimated for the sample column.

The response quantities for the performed analyses are expressed in terms global behaviour, i.e. axial loads, axial deformations, bending moment-axial load interaction and shear demand/capacity ratios. Additionally, lateral drifts at the column top were also computed along with the vertical displacement along the member axis. The results of the response history analyses are summarized hereafter.

AXIAL LOADS AND DEFORMATIONS OF BEAM-COLUMNS

Figure 10 provides the variations of axial load with respect to the static (gravity) load for the case of HGMs and HVGMs. Average values were computed and included in the plots. The results are provided for both North-South horizontal and East-West components of the earthquake. The variation of axial loads is significant in columns under HVGMs, especially in compression. For values of ν corresponding to actual RC columns in framed building structures, e.g., normalized axial load ν>0.10, the average increase of the compression load ranges between 174% (ν=0.20) and 59% (ν=0.50).

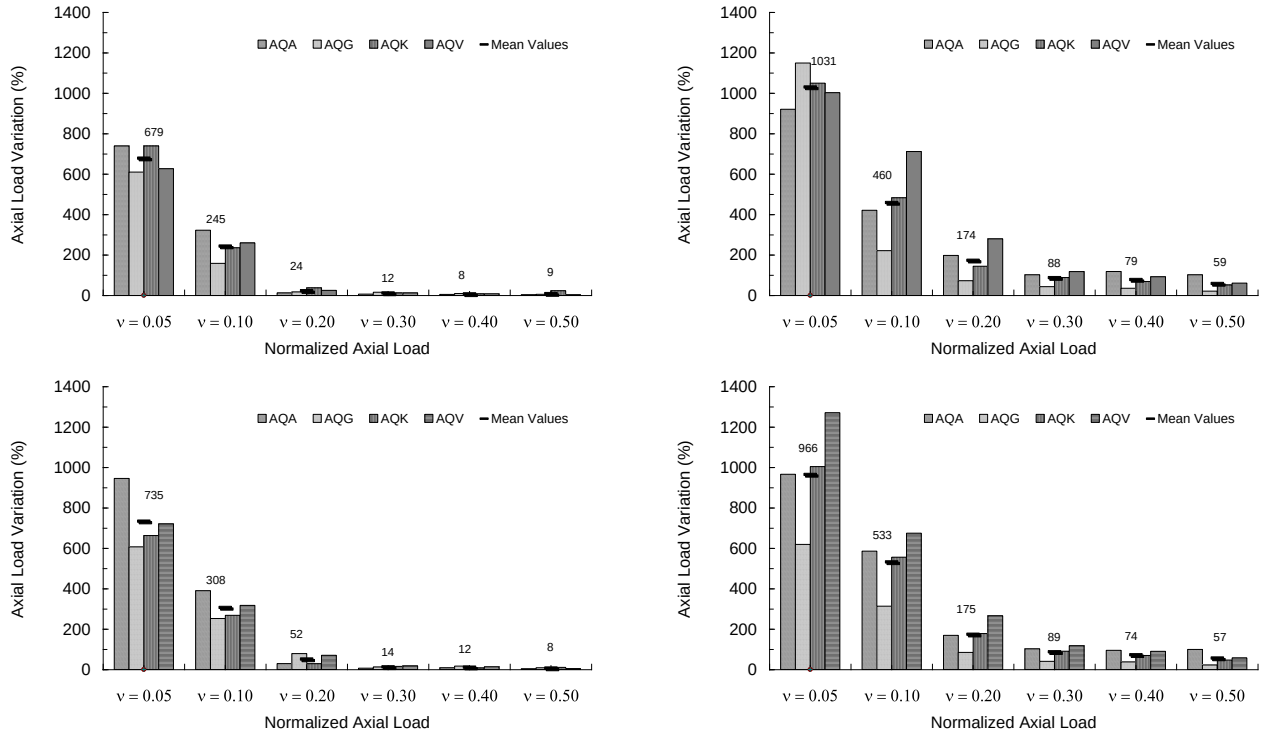

Figure 10 - Variation of axial loads in the column subjected to horizontal (*left*) and combined horizontal and vertical (*right*) earthquake ground motion: North-South (*top*) and East-West (*bottom*) horizontal components.

The results in Figure 10 also prove that in beam-columns subjected to horizontal seismic loads only, as the normalized axial loads ν become higher than 20, the axial load variations due to earthquake-induced vibrations are significantly lowered and can be neglected (see also Figure 11, where the axial load response history is provided for the North-South component of AQA record). This finding demonstrates the importance of including the effects of VGMs to estimate accurately the fluctuations of axial loads in the columns with respect to the gravity loads.

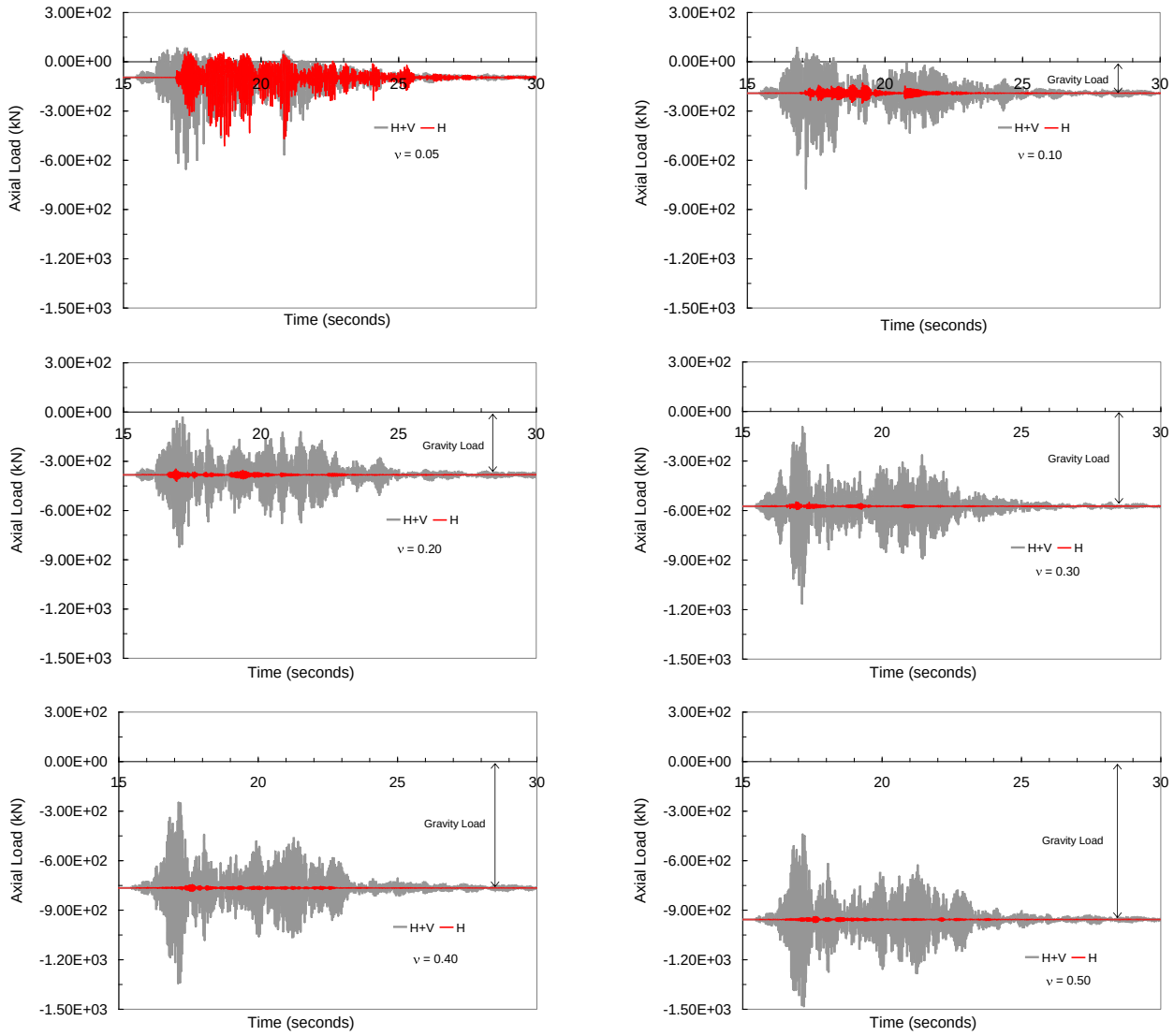

Figure 11 – Response history of the axial loads in the column subjected to horizontal (*left*) and combined horizontal and vertical (*right*) earthquake ground motion (North-South horizontal component, AQA record).

The comparison between the variations of axial loads in the RC columns considering the HGMs and the HVGMs is also summarised in Table 3 for the North-South components of the sample records.

	Normalized axial load (*design value*)					
Earthquake Component	$\nu = 0.05$	$\nu = 0.10$	$\nu = 0.20$	$\nu = 0.30$	$\nu = 0.40$	$\nu = 0.50$
Horizontal	679%	245%	24%	12%	8%	9%
Horizontal + Vertical	1031%	460%	174%	88%	79%	59%
(H+V) / H	1.52	1.88	7.25	7.33	9.88	6.56

Table 3 – Comparison between the variation of axial load considering the horizontal and horizontal+vertical component.

Note: The values refer to the North-South components. Gravity loads are assumed as benchmark for the variations.

The values listed in the table express the variations of the axial loads caused by the seismic loading with reference to the gravity load values. As the normalized axial load increases, e.g., ν>0.05, the variation of the axial loads tends to increase when the vertical component is implemented in the model used for the structural analysis. The values computed for the columns subjected to the combined horizontal and vertical seismic input can be higher than 7 times those computed for the horizontal component of the earthquake loading. The variations in Table 3 depend significantly on the level of axial load in the column. Net tensile forces may also occur in the columns as shown in Table 4. The results in the table indicate the cases where tensile forces were observed in the response history analyses carried out with different levels of normalized (design) axial load. For low values of normalized axial loads, e.g., $\nu \leq 0.10$, tensile actions occurred for all components of earthquake ground motions. For $\nu \geq 0.30$, which corresponds to the level of axial loads in ordinary low-to-medium rise RC framed buildings, tensile forces did not occur for all but the AQV records (when HVGMs are considered). For very high values of axial loads, e.g., $\nu \geq 0.40$, the sample columns are in compression.

The outcomes summarised in Table 4 are of paramount importance for the reliable earthquake assessment of RC members; it is shown that if vertical components are not accounted for in the seismic assessment of structural systems, tension response is not detected. RC members and structures may experience additional tension due to overturning, and as a result, may give rise to brittle failure mechanisms. The shear capacity of members is significantly affected by the reduction of axial load and the presence of tension, if any. Shear capacity is generally enhanced by the presence of compression actions (e.g., Paulay and Priestley, 1992), as further discussed later.

		Normalized Axial Load (ν)					
Station	Component	0.05	0.10	0.20	0.30	0.40	0.50
AQA	NSC						
	EWC						
	NSC+UDC						
	EWC+UDC						
AQG	NSC						
	EWC						
	NSC+UDC						
	EWC+UDC						
AQK	NSC						
	EWC						
	NSC+UDC						
	EWC+UDC						
AQG	NSC						
	EWC						
	NSC+UDC						
	EWC+UDC						

Table 4 – Occurrence of tensile action in the sample column.
Note: NSC = North-South component; EWC = East-West component; UDC = vertical (up-down) component.
Shaded areas indicate the cases where tension occurred.

Results similar to the above were found when the normalized axial loads computed with the actual mechanical properties, i.e., without accounting for partial safety factors (PSFs), see Table 2, were employed. Comparing the values in Tables 3 and 5, it is noted that the variations relative to actual values of the normalized axial loads are higher than those in Table 3. The variations relative to the preload (or gravity load) in the sample column are higher for the case of design normalized axial load; this finding was expected because load fluctuations are higher for lower axial loads (design versus actual normalized values).

The values of the axial loads in the columns induced by the HGMs and HVGMs are further compared in Figure 12. The results were derived using all sample earthquake records, i.e., AQA, AQG, AQK and AQV. Mean values and linear interpolations were also estimated to investigate the correlations, if any, between the sample data. Two observations are worth mentioning. The values of the axial loads relative to the columns subjected to HVGMs are significantly higher than those computed without the vertical components. By utilizing only the HGMs, the errors in the estimation of the axial loads can be as high as 300%.

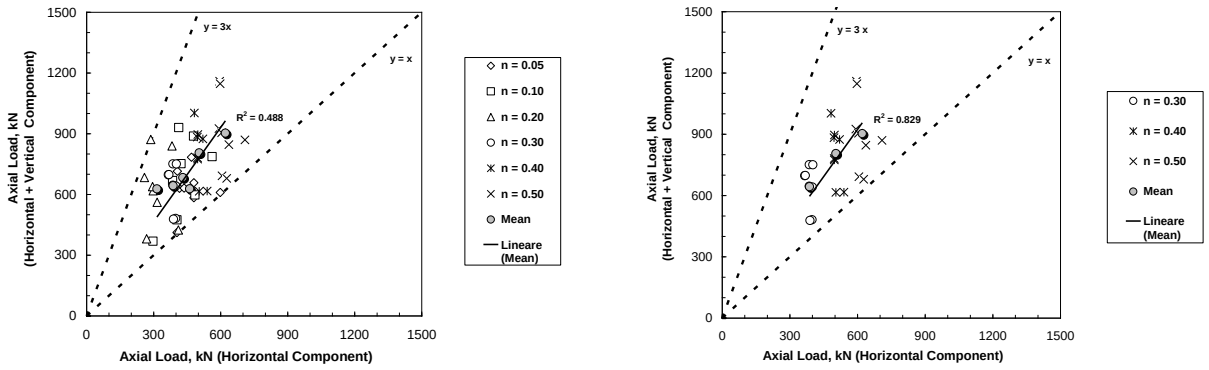

Figure 12 – Correlation between the axial loads in the column with and without the vertical component of earthquake ground motion (design normalised axial loads): all values of axial loads (*left*) and only high values of axial loads (*right*).

The computed results show that the underestimation has a linear trend as shown by the interpolation of the mean values included in the plot in Figure 12. However, the dispersion of the sample data is high as demonstrated by the low value of the linear regression coefficient (R^2), i.e., $R^2 = 0.448$. Results at low values of axial loads are less correlated than those at high values of axial loads. This response is due to the large fluctuations caused by the occurrence of cracking (see also Table 4). If intermediate and high ν-values are considered, the correlations between the above data improve significantly; the coefficient R^2 is 0.829, also displayed in Figure 12.

	Normalized axial load (*actual value*)					
Component	$\nu = 0.05$	$\nu = 0.10$	$\nu = 0.20$	$\nu = 0.30$	$\nu = 0.40$	$\nu = 0.50$
Horizontal	309%	66%	11%	6%	5%	4%
Horizontal + Vertical	512%	238%	86%	61%	44%	34%
(H+V) / H	1.66	3.60	7.82	10.17	8.80	8.50

Table 5 – Comparison between the variation of axial load considering the horizontal and horizontal+vertical component.

Note: The values refer to the North-South component. Gravity loads are assumed as benchmark for the variations.

Higher correlation for high values of the normalized axial loads was determined when the actual loads were employed in the analyses (see Figure 13). The computed results confirm the large variations (about 300%!) for the maximum axial loads occurring in the columns, under combined vertical and horizontal components of earthquake ground motions.

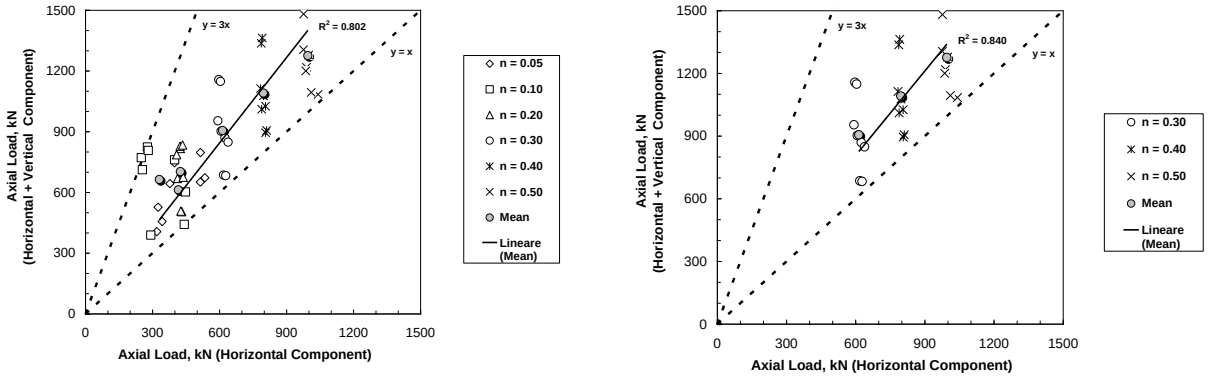

Figure 13 – Correlation between the axial loads in the column with and without the vertical component of earthquake ground motion (actual normalised axial loads): all values of axial loads (*left*) and only high values of axial loads (*right*).

Statistical analyses of the axial load variations in the columns were carried out and the results are expressed as a function of the axial load in Table 6. The computed values indicate the maximum fluctuations of the axial loads; they are estimated as a ratio of the earthquake-to-gravity load values. It is observed that coefficients of variation (COVs) for horizontal components is about 10%, while it is about 20% in the case of HVGMs. Nevertheless, the mean values prove that neglecting the vertical components may lead to underestimations of al least 60% (1.58 for $\nu = 0.50$).

		Normalized Axial Load					
		$\nu = 0.05$	$\nu = 0.10$	$\nu = 0.20$	$\nu = 0.30$	$\nu = 0.40$	$\nu = 0.50$
H	Mean (μ)	8.05	3.76	1.37	1.13	1.10	1.08
	Standard Deviation (σ)	1.11	0.69	0.24	0.04	0.04	0.07
	COV (σ / μ)	0.14	0.18	0.17	0.04	0.04	0.06
H + V	Mean (μ)	10.96	5.96	2.74	1.87	1.76	1.58
	Standard Deviation (σ)	1.89	1.71	0.76	0.32	0.30	0.31
	COV (σ / μ)	0.17	0.29	0.28	0.17	0.17	0.20

Table 6 – Maximum variations of the axial loads in the sample columns expressed as the ratio of the earthquake-to-gravity load values (EQL/GL).
Note: The values refer to all earthquake records. Gravity loads are assumed as benchmark values.

The underestimations of the axial load fluctuations for the cantilever systems are further summarized in Table 7, where the maximum variations in the sample columns are expressed as the ratio of the effects of HVGMs and VGMs. Scattered data were estimated for the mean values. However, the values are on average greater than 50%, thus supporting the need to include the effects of the vertical ground motions in the seismic performance assessment of RC members and structures.

	Normalized Axial Load					
	ν = 0.05	ν = 0.10	ν = 0.20	ν = 0.30	ν = 0.40	ν = 0.50
Mean (μ)	37.70	58.44	104.20	66.52	60.46	46.35
Standard Deviation (σ)	27.74	38.34	63.92	30.03	30.78	33.28
COV (σ / μ)	0.74	0.66	0.61	0.45	0.51	0.72

Table 7 – Maximum variations of the axial loads in the sample columns expressed as the ratio of the effects of horizontal+vertical and vertical ground motions ((H+V)/H).
Note: The values refer to all earthquake records. Values due to horizontal components are assumed as benchmark values. Mean values and standard deviations are expressed in percentage.

Significant fluctuations of axial loads were also computed for the central columns of the sample RC frame, as shown in Figures 14 and 15. It is observed that net tensile forces were computed at both ground and first floors when the frame was subjected to the AQA records. Large vertical accelerations on the central columns of multi-storey RC frames are due primarily to the low overturning effects and the large translation masses acting on such columns. For exterior columns of the plane frame the variations of axial loads when HVGMs are considered is negligible.

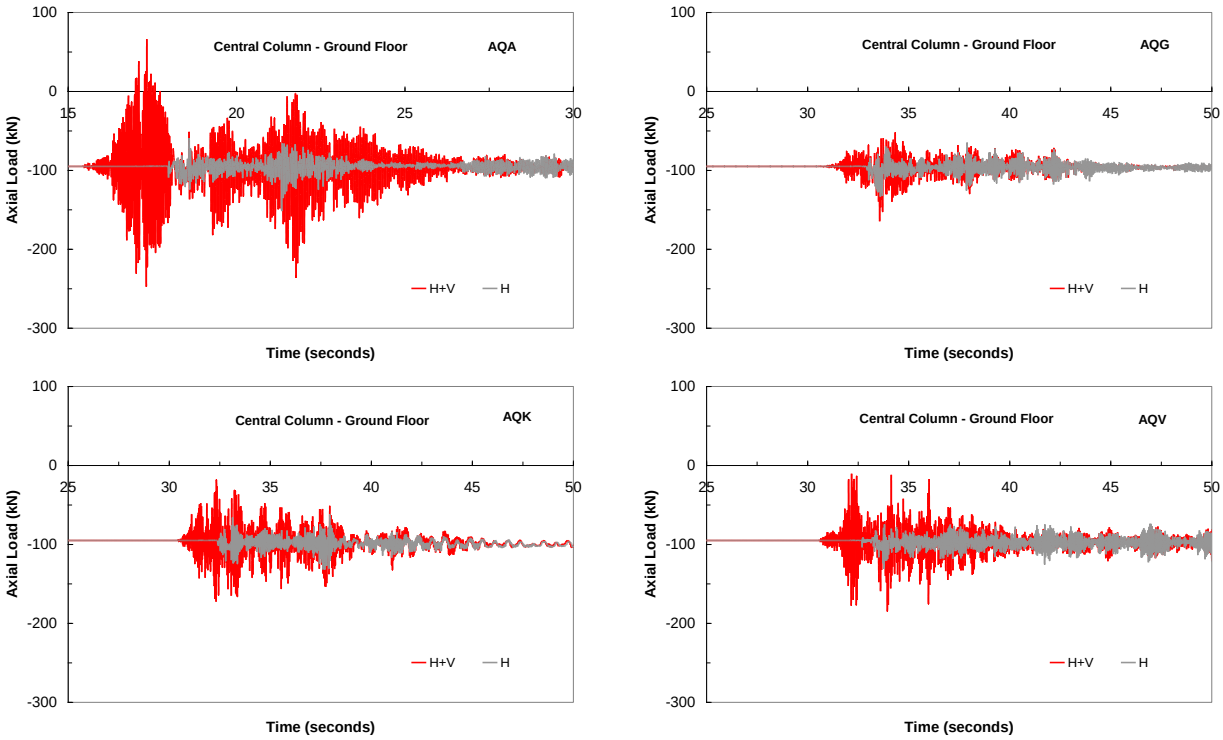

Figure 14 – Response history of the axial loads in the central column at the ground floor of the plane frame subjected to horizontal (*left*) and combined horizontal and vertical (*right*) earthquake ground motions (north-south horizontal component)..

The extensive numerical simulations carried out in the present study demonstrate that the axial deformations of the beam-column model are underestimated if VGMs are not accounted for. Vertical oscillations due to the axial-bending coupling during seismic response of the columns were observed, especially for elements with low axial loads. Similar response was derived by Ranzo *et al*. (1999). The computed variations of the axial deformations are displayed in Figure 16 for the sample RC columns.

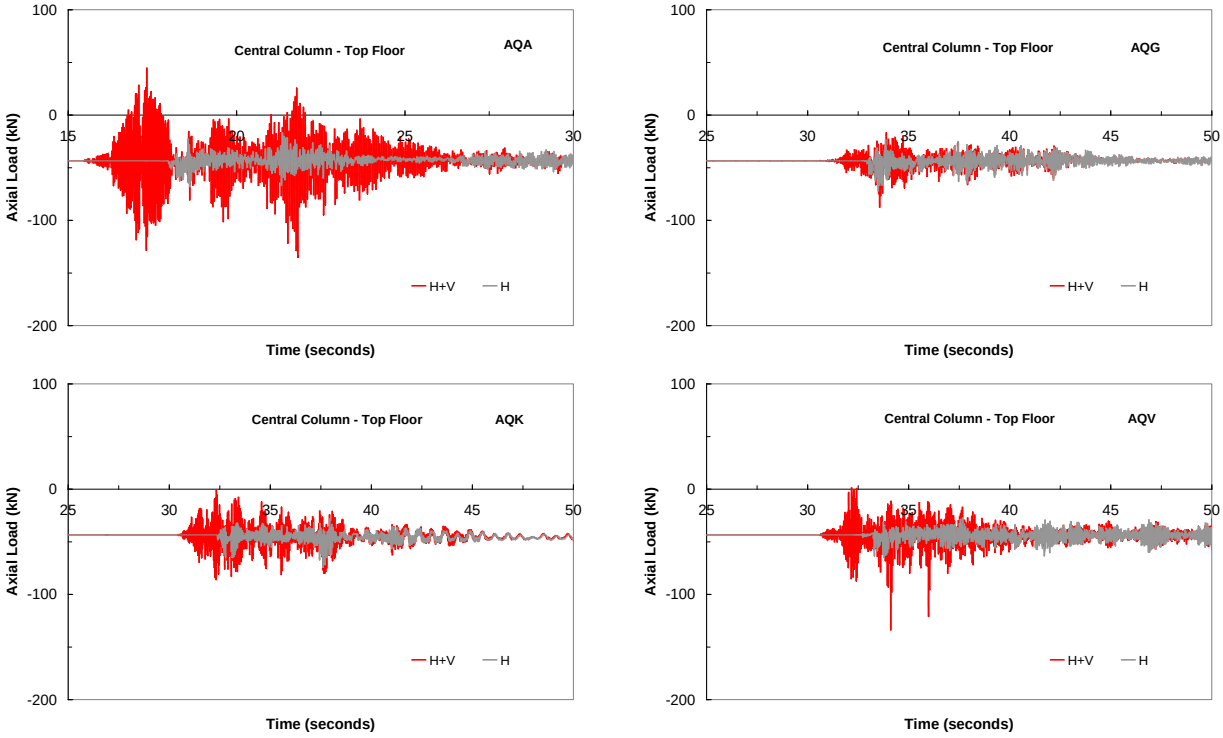

Figure 15 – Response history of the axial loads in the central column at the first floor of the plane frame subjected to horizontal (*left*) and combined horizontal and vertical (*right*) earthquake ground motion (North-South horizontal component, AQA record).

The deformations increase significantly in compression with respect to the initial deformation caused by gravity loads in the column. When the vertical component of earthquake ground motion is included in the analyses, the variations of axial deformations are significantly higher (for ν=0.20, it is about 620% for East-West component and 1660% for North-South component) with respect to the static deformations. The minimum variation is 76% when the VGM is considered, which is about 5 times the value computed when using the horizontal component only (76% versus 17%). The comparisons between the axial deformations in Table 8 confirm the outcomes derived for the axial load variations (see Table 3). Increased axial load deformations in compression may give rise to concrete crushing and may reduce the (flexural-

axial load interaction) capacity of RC members as further discussed later. Tensile deformations were computed for low load values of normalized axial loads, e.g., $\nu \leq 0.10$.

	Normalized axial load (design value)					
Component	$\nu = 0.05$	$\nu = 0.10$	$\nu = 0.20$	$\nu = 0.30$	$\nu = 0.40$	$\nu = 0.50$
Horizontal	1151%	329%	26%	15%	14%	17%
Horizontal + Vertical	3034%	618%	201%	128%	100%	76%
(H+V) / H	2.64	1.88	7.73	8.33	7.14	4.47

Table 8 – Comparison between the variations of axial deformations considering the horizontal and horizontal+vertical component.

Note: The values refer to the North-South component. Gravity loads are assumed as benchmark for the variations.

The correlations between the axial deformations due to the horizontal and combined horizontal and vertical components of earthquake ground motions were also evaluated. The results are displayed in Figure 16 for all sample records. Axial deformations have higher correlations with respect to the axial loads. The regression coefficient is $R^2 = 0.820$, when the design normalized axial loads are considered. If the actual normalized axial loads are utilized, the correlation is enhanced ($R^2 = 0.900$ versus $R^2 = 0.820$) as also shown in Figure 16.

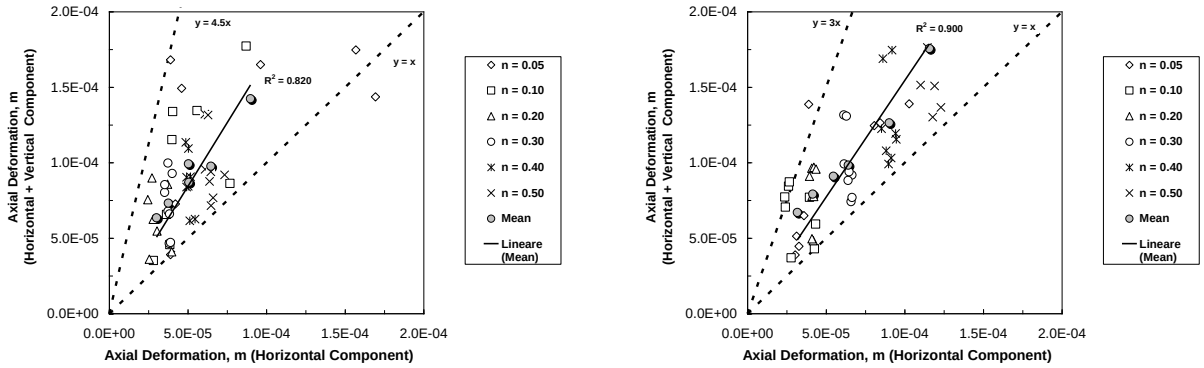

Figure 16 – Correlation between the axial deformations in the column with and without the vertical component of earthquake ground motion: design (*left*) and actual (*right*) normalized axial loads.

Mean values and standard deviations of the axial deformations in the columns were evaluated; the results are expressed as a function of the axial load in Table 9. For low values of axial loads there is a large scatter when either the horizontal or the combined HVGMs are accounted for. However, as the axial load increases, variations of the axial deformations under the horizontal earthquake tend to decrease; the interaction between the axial load and the bending moment lowers the axial deformations. The vertical component exacerbates the seismic performance by further increasing the axial deformations.

		Normalized Axial Load					
		$\nu = 0.05$	$\nu = 0.10$	$\nu = 0.20$	$\nu = 0.30$	$\nu = 0.40$	$\nu = 0.50$
H	Mean (μ)	17.12	4.77	1.41	1.16	1.16	1.16
	Standard Deviation (σ)	10.65	2.00	0.26	0.05	0.04	0.07
	COV (σ / μ)	0.62	0.42	0.18	0.04	0.04	0.06
H + V	Mean (μ)	27.16	9.42	2.99	2.27	1.99	1.76
	Standard Deviation (σ)	11.36	4.68	0.92	0.62	0.43	0.41
	COV (σ / μ)	0.42	0.50	0.31	0.27	0.22	0.23

Table 9 – Maximum variations of the axial deformations in the sample columns expressed as the ratio of the earthquake-to-gravity load values (EQL/GL).
Note: The values refer to all earthquake records. Gravity loads are assumed as benchmark values.

A comparison between the effects of HGMs and HVGMs is provided in Table 10, in which the mean values, the standard deviations and the COVs for the computed values are included. The assessment of the column response showed significant residual deformations for values of ν>0.20 (Figure 17); these deformations generate column shortenings. The latter have been found to impair the seismic performance of steel framed structures (e.g. Como *et al*., 2003; MacRae, 2006, among many others). In RC framed structures the aforementioned shortening may increase the seismic demand imposed on beam elements. However, the influence of the column shortening should not be very significant for the seismic response of RC building structures. Research is still ongoing.

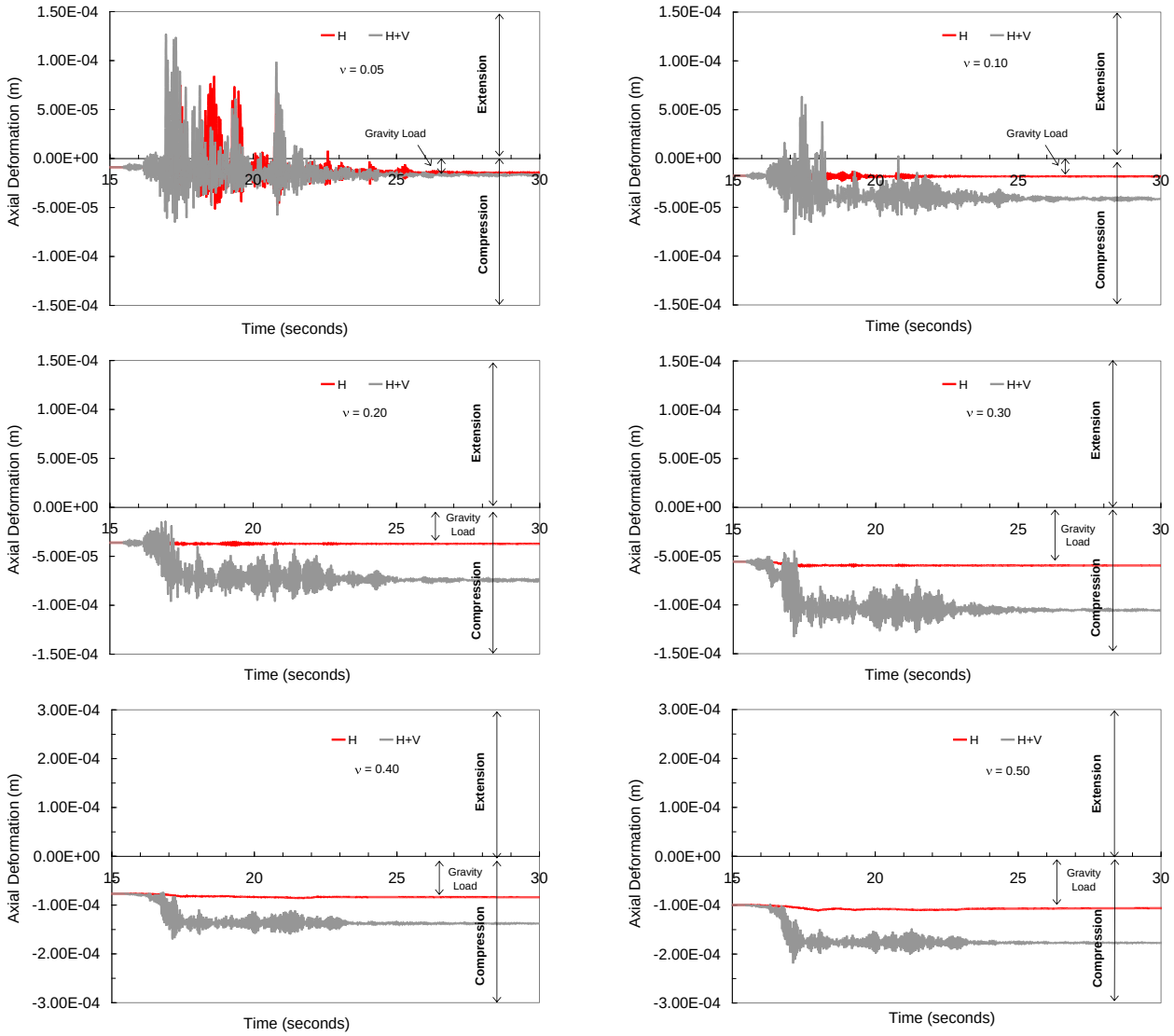

Figure 17 – Response history of the axial deformations in the column subjected to horizontal (*left*) and combined horizontal+vertical (*right*) earthquake ground motion (North-South horizontal component, AQA record).

	Normalized Axial Load					
	ν = 0.05	ν = 0.10	ν = 0.20	ν = 0.30	ν = 0.40	ν = 0.50
Mean (μ)	96.54	100.60	117.78	96.03	73.09	52.53
Standard Deviation (σ)	121.00	82.24	77.08	55.37	41.28	40.71
COV (σ / μ)	1.25	0.82	0.65	0.58	0.56	0.78

Table 10 – Maximum variations of the axial deformations in the sample columns expressed as the ratio of the effects of horizontal+vertical and vertical ground motions ((H+V)/H).
Note: The values refer to all earthquake records. Values due to horizontal components are assumed as benchmark values. Mean values and standard deviations are expressed in percentage.

The axial residual deformations were also detected from the vertical displacements of the cantilever top, as shown in Figure 18, in which the response histories of the vertical displacements for the AQA records (North-South component) are provided as a function of the

normalized axial loads. For values of normalized loads $\nu \geq 0.20$, the columns are characterised by similar dynamic response. The magnitude of the residual displacement and the time required to damp the vibrations depends on the level of axial loads. The higher the values of ν, the more uniform the axial response of the structural member. Similar results were computed for AQG, AQK and AQV records.

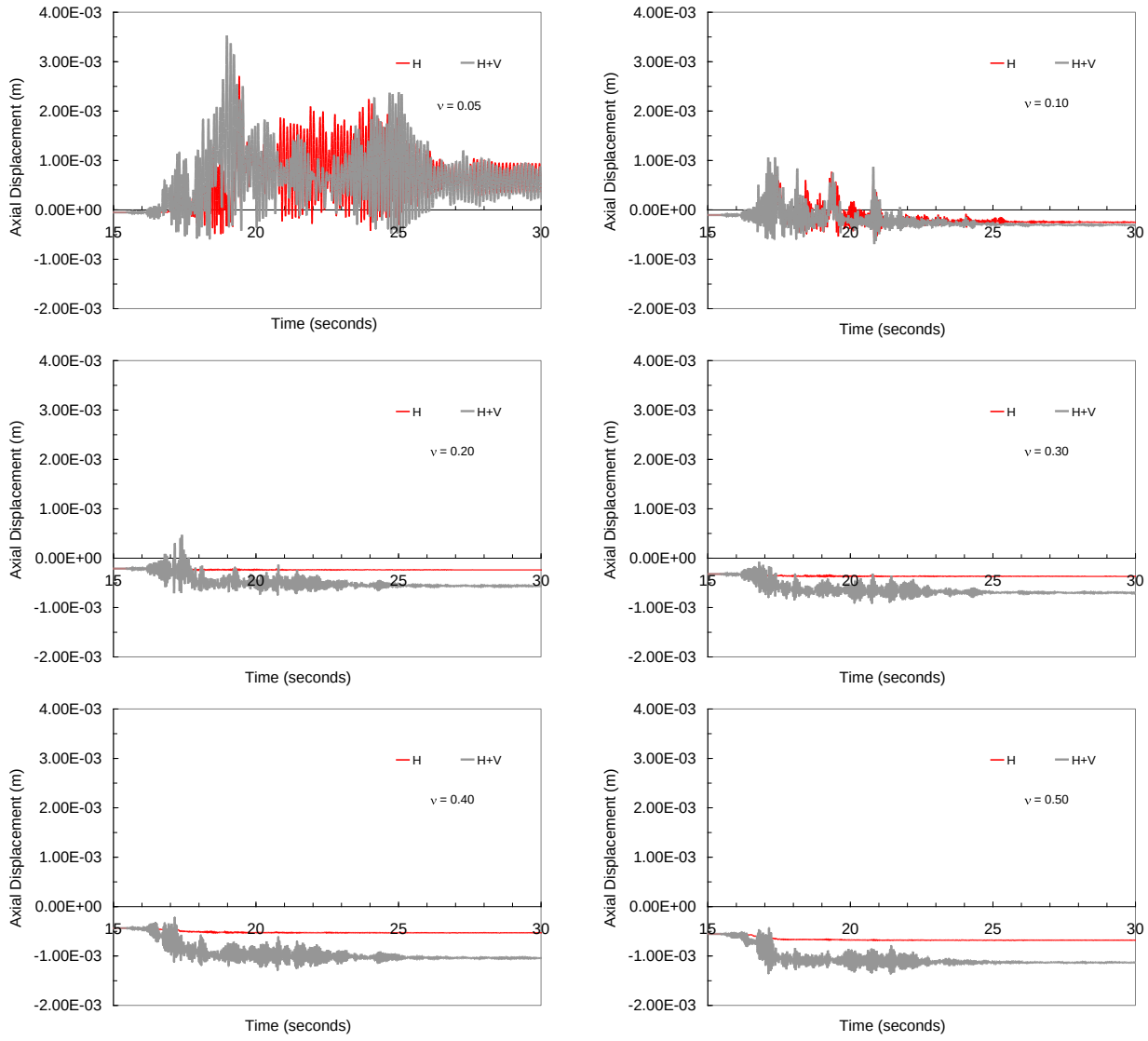

Figure 18 – Axial displacements (AQA record: North-South component) response history.

The residual axial deformations in the columns subjected to combined horizontal and vertical components of ground motion are significantly affected by the level of normalized axial loads and earthquake characteristics (see Figure 19). The average increase of the initial axial deformation due to gravity loads is about 60% for normalized loads $\nu \geq 0.20$.

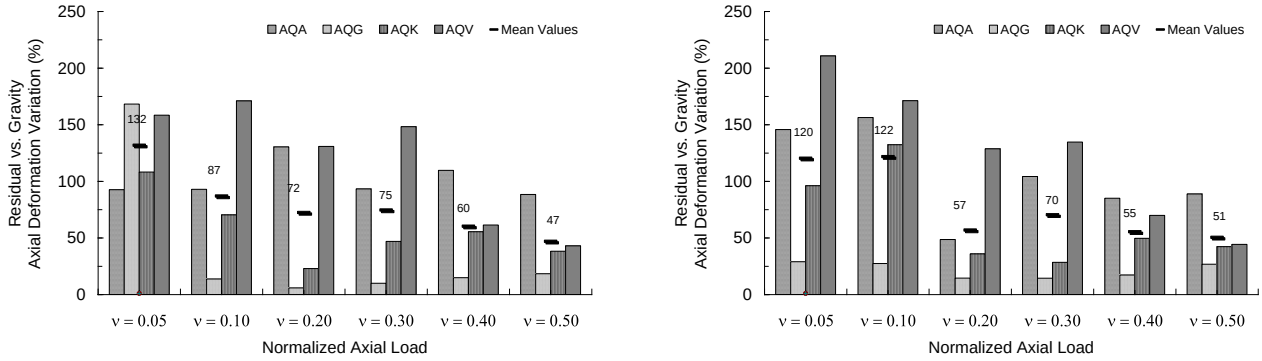

Figure 19 - Variation of the residual (compression) axial deformations in the column subjected to combined horizontal and vertical earthquake ground motion: North-South (*left*) and East-West (*right*) horizontal component.

BENDING MOMENT-AXIAL LOAD INTERACTIONS

The strength capacity of the sample columns was also assessed in terms of bending moment-axial load interaction. Shear response of RC members was also considered and is discussed in the next paragraph. Interaction domains (N, M) were computed and employed as benchmarks to assess and compare the seismic demand. Both design and actual material properties were utilized for the derivations of the (N, M) domains. Figures 20 and 21 display the computed interaction curves and the pairs (N, M) evaluated for the South-North and East-West components for the AQA records, respectively.

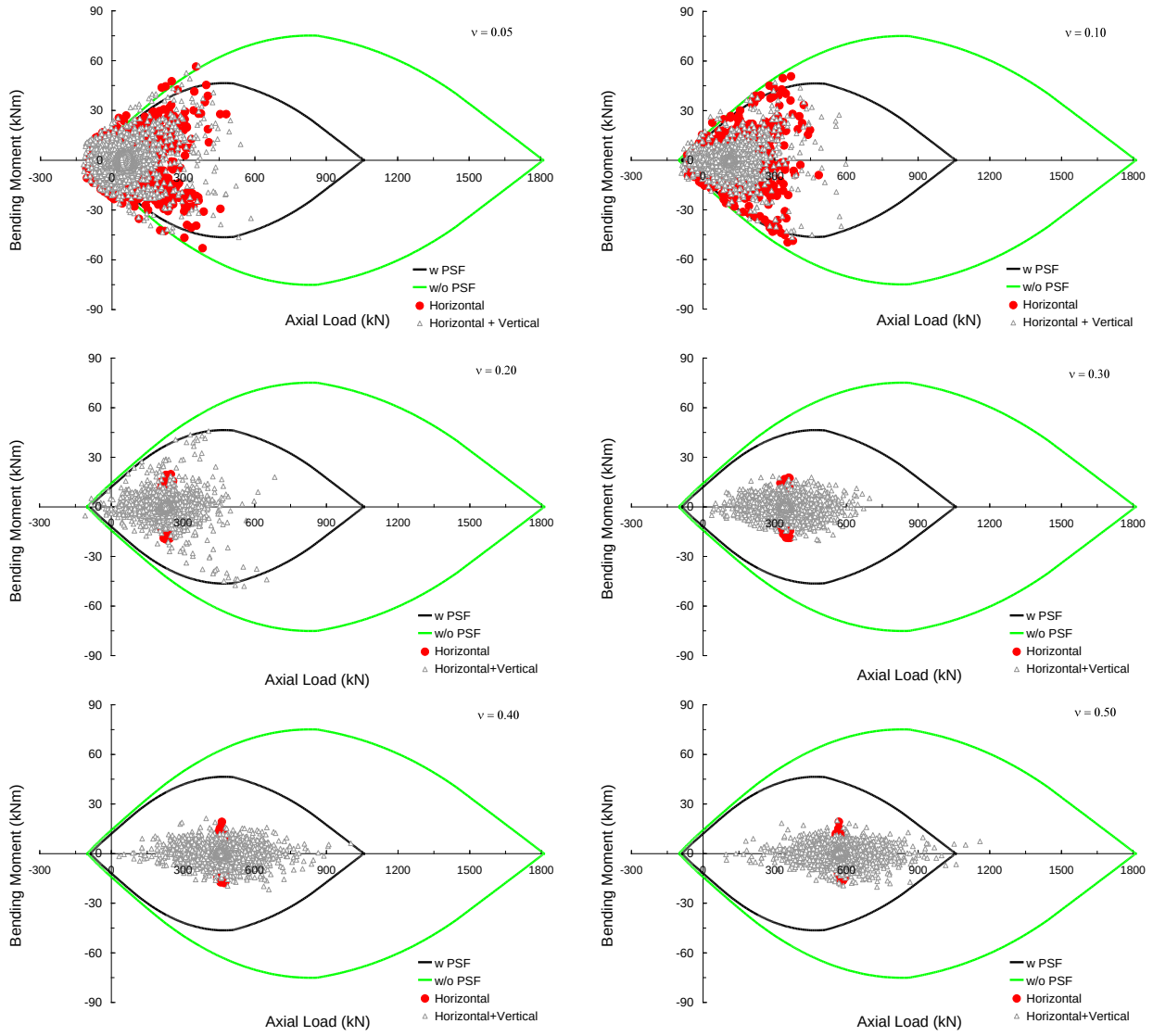

Figure 20 – Bending moment–axial load interaction (AQA record: North-South component): column preloaded with design normalized axial loads.

The results are significantly affected by the value of the axial preload due to the gravity loads in the column. For normalized axial loads $\nu \leq 0.20$, the results show large variations; the latter are generated primarily by the large fluctuations of the bending moments. Cracking occurs at an early stage and lowers the flexural capacity of RC members. The dots in plots of the interaction domains are located on the left hand side, i.e., towards the area characterized by tension. Scattered results were derived for both HGMs and HVGMs. As the axial loads increase, e.g., $\nu > 0.20$, the (N, M) pairs exhibit low variations when compared to vertical components of ground motions. Similar results were derived for the actual values of normalized axial loads (Figure 22).

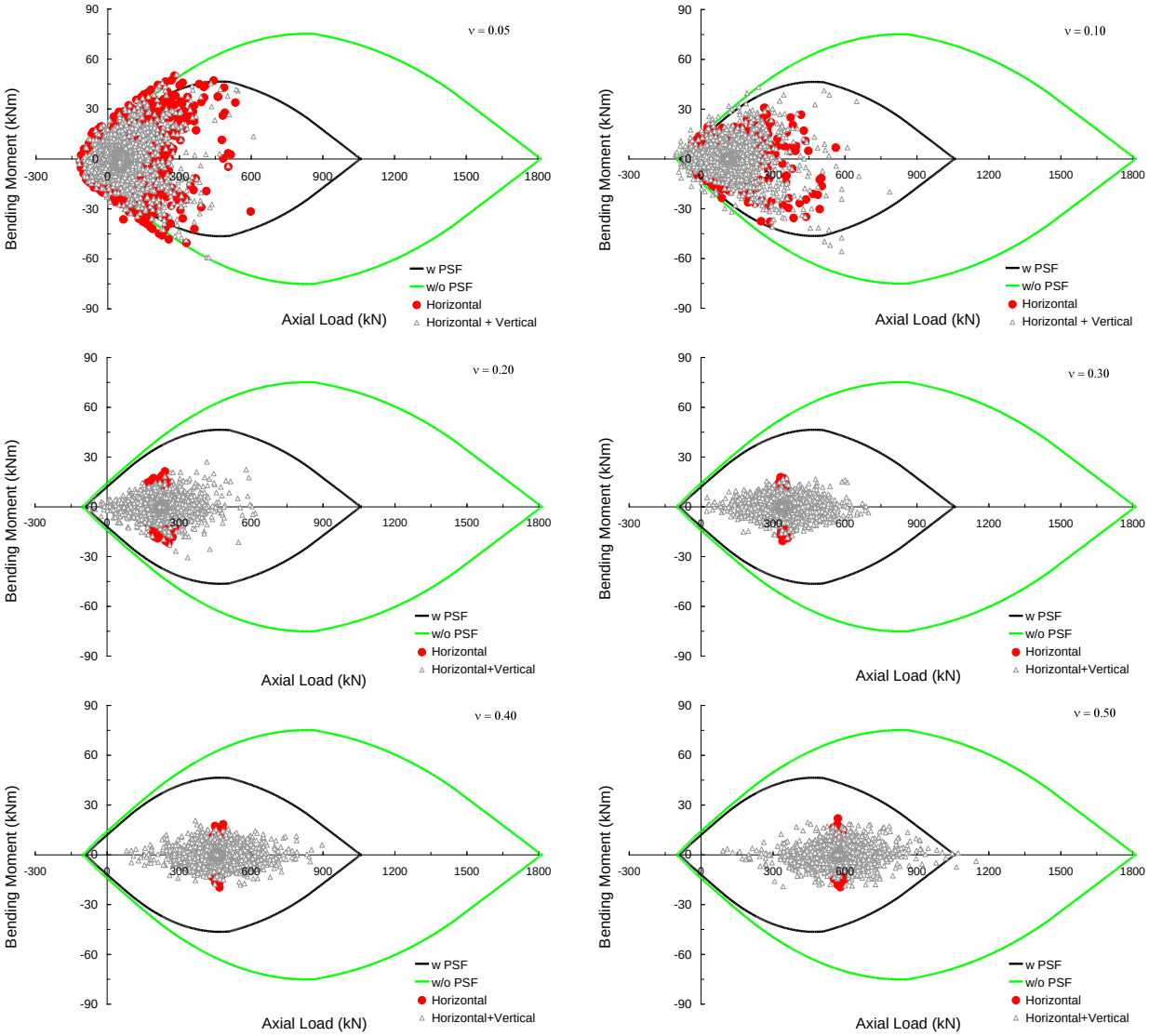

Figure 21 – Bending moment–axial load interaction (AQA record: East-West component): column preloaded with design normalized axial loads.

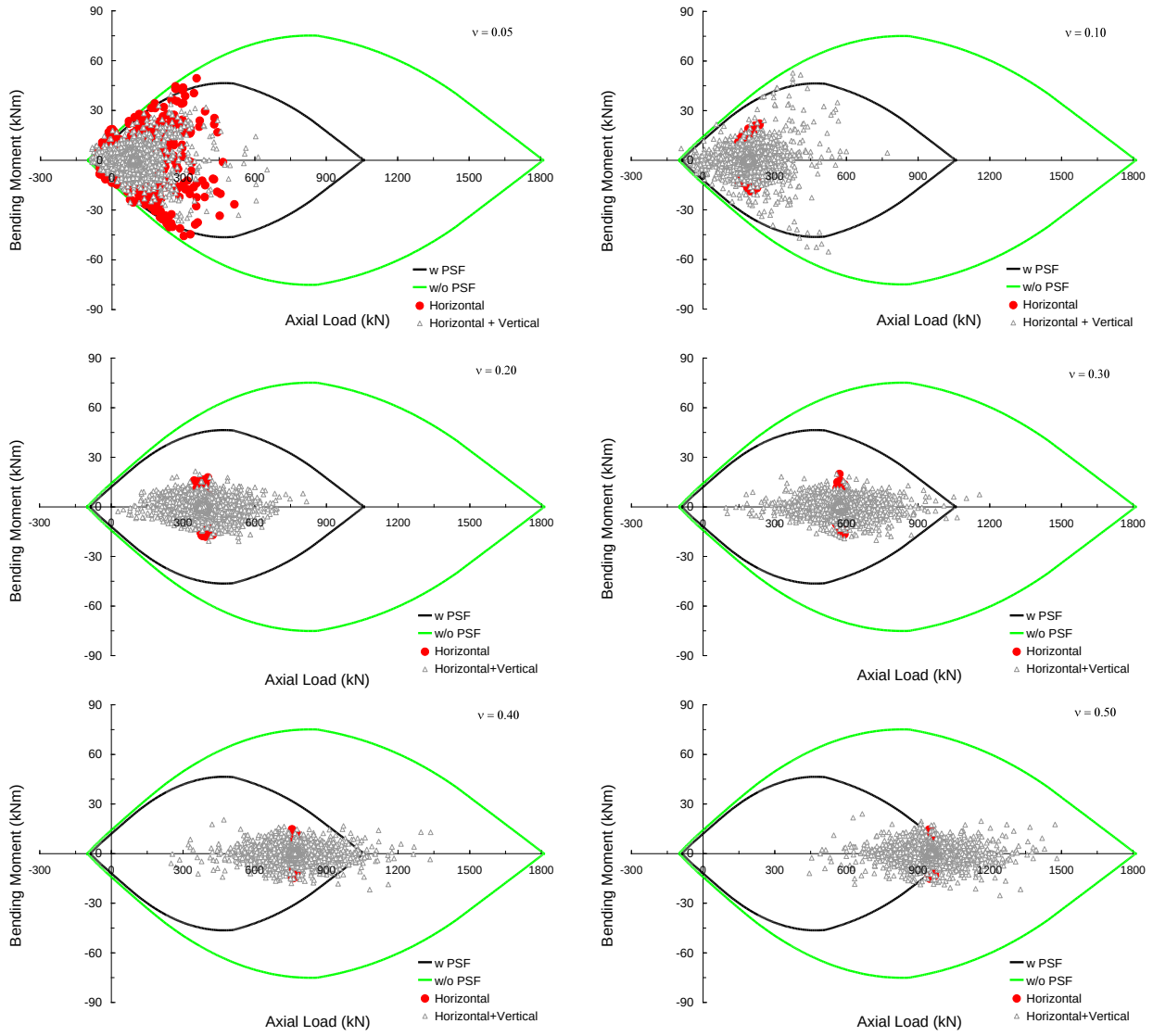

Figure 22 – Bending moment–axial load interaction (AQA-North-South component): actual normalized axial loads.

The effects of the bending moment are more significant when the horizontal earthquakes only are employed. These results support the findings of previous research by Ranzo, et al. (1999), Button, et al. (2003) and Kunnath, et al. (2005) for RC bridge piers. The distribution of the (N, M) pairs in the domains given in Figures 20 to 23 shows that when HGMs are employed the variation of the bending moment tends to be higher than in the case of combined horizontal and vertical earthquake loading. In this case, the variation of the axial load exceeds considerably the bending moment fluctuations.

For high values of normalized axial loads the computed (N, M) pairs lie beyond the threshold interaction curves and, in turn, the RC member fails. The importance of including the

vertical earthquake loading in the seismic assessment is evident form the results plotted in Figures 20 and 21. Similar response was evaluated for the actual normalized axial loads; the results are less scattered because of the higher values of axial loads (Figure 22). However, the estimations are yet unsafe when the vertical earthquake loading is neglected.

The statistical analysis of the maximum bending moments due to the horizontal and combined horizontal and vertical components of earthquake loading in the sample RC cantilever columns shows that the variations of such moments are low. Mean values in Table 11 show that the variation is generally less than 10%.

SHEAR RESPONSE

The most brittle failure mode of RC members is shear collapse, especially for beam-columns. Shear failure is caused by the lack of lateral reinforcement, e.g., size, spacing and strength of transverse reinforcement. The shear response of RC columns under earthquake loading is not yet fully understood. Variation in axial loading is critical with respect to the shear strength. A limited number of experimental studies have addressed the problem of changing axial loads in columns subjected to earthquake loading, wherein the typical loading history was that high shear in the column was accompanied by high compression and low shear by low compression or tension (Penelis and Kappos, 1997). The fluctuations of axial loads in RC columns influence detrimentally their stiffness, strength and ductility. The lateral stiffness is significantly lowered when the axial force varies, but it remains constant after yielding. The displacement increases rapidly with decreasing axial load, because previously opened cracks do not close. Longitudinal steel reinforcement bars subjected to tensile strains during cycles of increasing axial compression may accumulate progressive plastic strains. Decreasing compression and/or tension reduces the moment capacity.

	Normalized Axial Load					
	$\nu = 0.05$	$\nu = 0.10$	$\nu = 0.20$	$\nu = 0.30$	$\nu = 0.40$	$\nu = 0.50$
Mean (μ)	7.94	7.60	26.61	-0.67	6.89	1.63
Standard Deviation (σ)	20.27	18.84	50.63	6.93	6.36	8.17
COV (σ / μ)	2.55	2.48	1.90	-10.27	0.92	5.01

Table 11 – Maximum variations of the bending moments in the sample columns expressed as the ratio of the effects of horizontal+vertical and vertical ground motions ((H+V)/H).
Note: The values refer to all earthquake records. Values due to horizontal components are assumed as benchmark values. Mean values and standard deviations are expressed in percentage.

The shear strength of RC members under earthquake loading is affected by a number of parameters: level of axial force, applied shear stress level, level of imposed ductility, aspect ratio, transverse steel ratio and longitudinal steel ratio. The above parameters are accounted for differently in the existing capacity models (e.g., FIB, 2003). To assess reliably the shear resistance, different capacity models for RC structural members were utilized in the present study. The numerous models that have been proposed to evaluate the shear strength assume that the resistance of RC members comprises a primary contribution of web reinforcement (the tension ties of the Ritter-Mörsh truss analogy) and secondary contributions. These are attributed to other mechanisms of resistance that are mobilized through diagonal tension of concrete web, i.e., the dowel action of longitudinal reinforcement spanning across cracks, the frictional interlock between cracked interfaces and reinforcement to concrete bond (tension-stiffening) along the bar between adjacent cracks.

First, the model for members with vertical shear reinforcement as implemented in CEN (2006-a) was employed. It is assumed that the shear resistance V_{Rd} is given by:

$$V_{Rd} = \min\left(V_{Rd,s}; V_{Rd,max}\right) \tag{1}$$

where the design value of the shear force $V_{Rd,s}$, which can be sustained by the yielding shear reinforcement, can be expressed as follows:

$$V_{Rd,s} = \frac{A_{sw}}{s} z\, f_{ywd} \cot\theta \tag{2}$$

and the design value of the maximum shear force $V_{Rd,max}$, which can be sustained by the member, limited by crushing of the compression struts, is:

$$V_{Rd,max} = \frac{\alpha_{cw}\, b_w\, z\, \nu_1\, f_{cd}}{\left(\cot\theta + \tan\theta\right)} \tag{3}$$

In the above relationships, A_{sw} is the cross-section area of the shear reinforcement, s is the spacing of the stirrups, z indicates the inner lever arm, for a member with constant depth, corresponding to the bending moment in the element under consideration. In the shear analysis of reinforced concrete without axial force, the approximate value $z = 0.9d$ may normally be used. θ is the angle between the concrete compression strut and the beam axis perpendicular to the shear force; α_{cw} is a coefficient taking account of the state of the stress in the compression chord; and b_w corresponds to the minimum width between tension and compression chords. The

design yield strength of the shear reinforcement is denoted as f_{ywd} and f_{cd} is the design compression strength of the concrete.

The value of the strength reduction factor for the concrete cracked in shear ν_1 is as below:

$$\nu = 0.6\left[1 - \frac{f_{ck}}{250}\right] \qquad (f_{ck} \text{ in MPa}) \qquad (4)$$

It is also assumed that $\alpha_{cw} = 1.0$, as recommended by CEN (2006-a).

The values of shear resistance $V_{Rd,max}$ for the sample cantilever columns corresponding to the angle of the strut $\theta = 22°$ or $\theta = 45°$ are 291.879kN and 423.225kN, respectively. These values of $V_{Rd,max}$ were determined assuming PSFs equal to unity. Such values are exceeded during the response history of the shear demand on the columns, hence the compressed struts fail.

The contribution of the concrete to the shear strength ($V_{RD,c}$) was also estimated to perform consistent comparisons with other formulations. The value of $V_{RD,c}$ is computed as follows:

$$V_{Rd,C} = \left[C_{RD,ck}\, k\,(100\,\rho_l\, f_{ck})^{1/3} + k_1\,\sigma_{cp}\right] b_w\, d \qquad (5)$$

with a minimum of:

$$V_{Rd,C} = \left(v_{min} + k_1 \sigma_{cp}\right) b_w\, d \qquad (6)$$

where f_{ck} is the concrete compression strength (in MPa); A_{sl} is the area of the tensile reinforcement, which extends $\geq (l_{bd}+d)$ beyond the section considered., N_{Ed} is the axial force in the cross-section due to loading (in N), with $N_{Ed} > 0$ in compression. A_c is the area of concrete cross section (in mm^2).

The parameters k and ρ_l in eqn.(5) are as follows:

$$k = 1 + \sqrt{\frac{200}{d}} \leq 2.0 \qquad (7)$$

with d in mm and:

$$\rho_l = \frac{A_{sl}}{b_w\, d} \qquad (8)$$

The normal stress due to the axial loads are:

$$\sigma_{cp} = \frac{N_{Ed}}{A_c} < 0.2\, f_{cd} \qquad \text{(in MPa)} \tag{9}$$

The value of the shear resistance $V_{Rd,C}$ is expressed in N. The coefficient $C_{Rd,c}$, k_1 and v_{min} are assumed equal to the recommended values provided in CEN (2006-a), i.e., $C_{Rd,c} = 0.18/\gamma_c$ and $k_1 = 0.15$ and $v_{min} = 0.035\, k^{3/2}\, fck^{1/2}$.

Comparisons for shear demand and supply in the cantilever columns are provided in Figure 23 for the North-South component of the AQA earthquake record. It is found that the shear supply is exceeded for all sample columns. Shear demand is higher for lower values (e.g. ν<0.10) of normalized axial loads. Columns with higher axial loads display less laterally and hence the base seismic shear demand is lowered. As the axial loads increase, the stiffness degradation and the strength deterioration are also minimized.

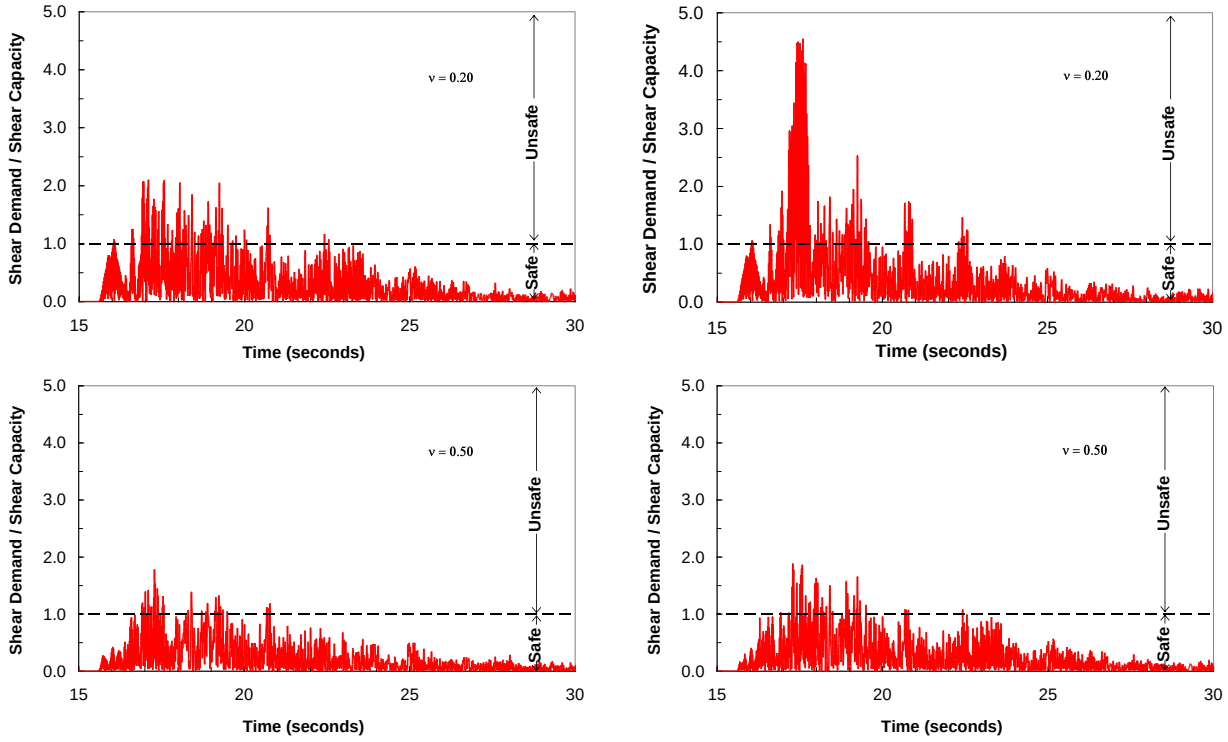

Figure 23 – Shear response (north-south component: AQA record): horizontal (*left*) and horizontal and vertical (*right*): design normalized axial loads.

However, for moderate-to-high values of axial loads, e.g., $\nu \geq 0.20$, with respect to the actual mechanical properties of the RC members, the shear resistance is reduced by the increase

of the axial loads. For a given level of axial loads, the effects of the vertical component of earthquake ground motion on RC structural members are two-fold. The shear demand is increased and the supply is lowered due to the great deterioration of the strength generated by the significant fluctuation of the axial forces. As a result, seismic performance of RC structures can be reliably assessed when both horizontal and vertical earthquake ground motions are considered.

Further assessment of shear forces was also carried out. The shear strength was determined using the formulas proposed by Paulay and Priestley (1992) for RC columns. The shear strength V_t at a section of the beam-column can be expressed as follows:

$$V_t = V_c + V_s \tag{10}$$

where the contribution of the concrete V_c to the shear strength is:

$$V_c = v_c \, b_w \, d \tag{11}$$

with b_w and d the width of the web and the effective depth of the cross-section, respectively. The term v_c, in regions of plastic hinges of columns can be expressed as below:

$$v_c = v_b \sqrt{\frac{N}{A_c \cdot f_c}} \tag{12}$$

and

$$v_b = 0.07 + 10\,\rho_w \sqrt{f_c} \le 0.2\sqrt{f_c} \qquad \text{(in MPa)} \tag{13}$$

where the ratio of the flexural tension reinforcement ρ_w is expressed in terms of the web width b_w. The above equations are applicable when the axial load N results in compression. Conversely, when the axial load N is in tension, then the shear stress $v_c = 0$.

The contribution of shear reinforcement V_s to the total shear V_t is derived assuming the truss model with 45° diagonal struts and hence:

$$V_s = \frac{A_{sw} \, f_{yw} \, d}{s} \tag{14}$$

where A_{sw}, f_{yw}, d and s indicate the same quantities as in eqn.(2) implemented in CEN (2006-a). The assessment of the capacity model proposed by Paulay and Priestley (1992) led to the same results estimated using the code approach. Results similar to those computed for the cantilever columns were also estimated for the central columns of the sample multi-storey plane frame.

It has been repeatedly reported (e.g. Papazoglou and Elnashai, 1996; Alaghebandian, et al., 1998; Alaghebandian, et al., 1999; Mwafy and Elnashai, 2006; Kim and Elnashai, 2008; Kunnath, et al., 2008) that storey shears and lateral (either floor or interstorey drifts) displacements are not influenced by the effects of the VGMs. The time histories of the base shears show that shear forces may be influenced by the vertical component of earthquake ground motion (Figure 24); such influence is a function of the preload. Differences may arise particularly for low values of the normalized axial loads due to the occurrence of cracking as displayed in Figure 24.

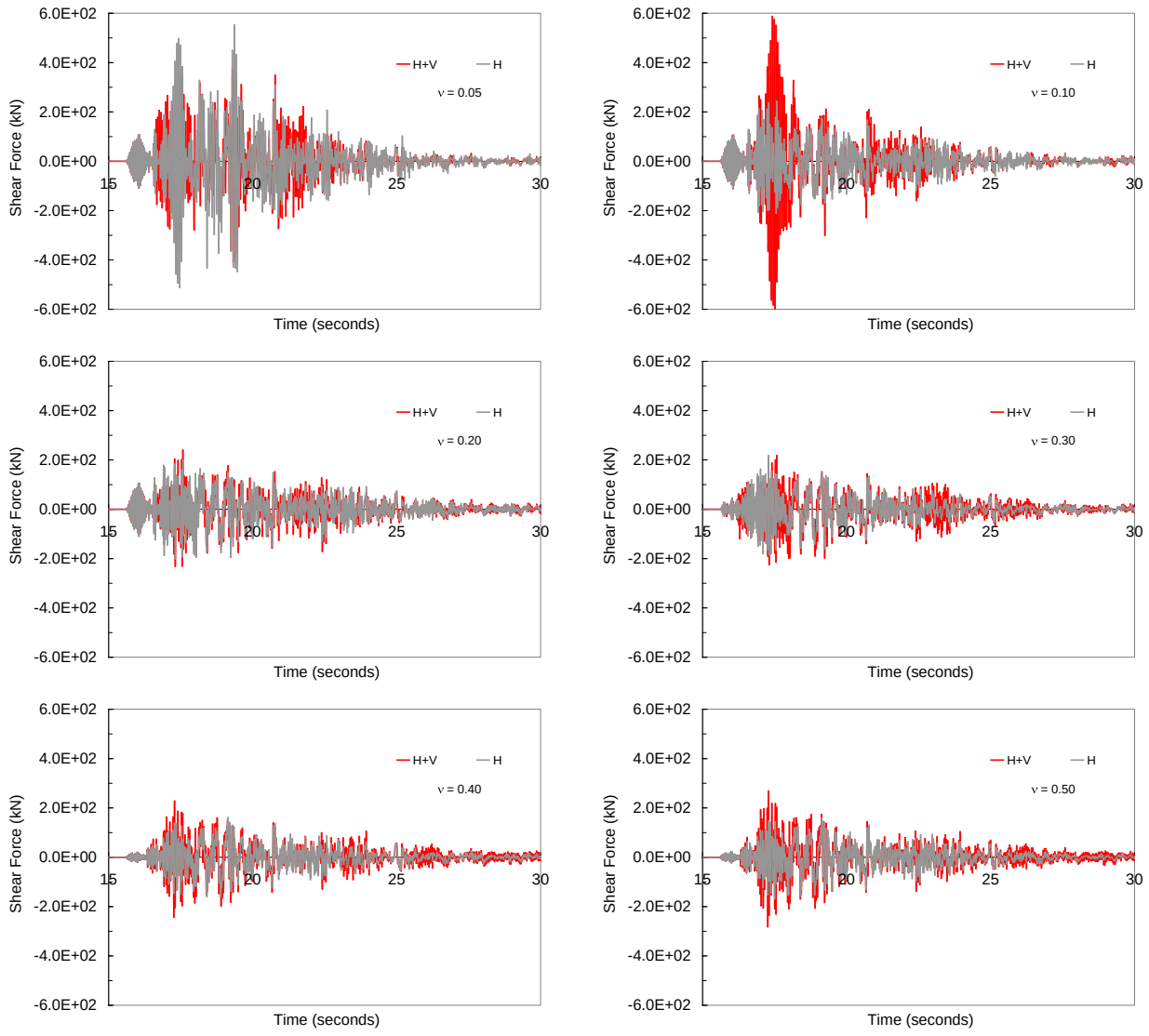

Figure 24 – Base shear time history response (AQA-North-South component).

CONCLUSIONS

The present work investigated the structural response of RC members and buildings subjected to horizontal (HGMs) and vertical (VGMs) ground motions recorded during the 6 April 2009 L'Aquila earthquake, in Italy. The emphasis was on the normalized axial loads in columns and the peak ground acceleration ratios between horizontal and vertical ground accelerations. Normalised axial loads and the ratios of $(PGA)_h/(PGA)_v$ are considered fundamental parameters for the assessment of structural components and systems subjected to combined horizontal and vertical ground motions (HVGMs).

The suite of earthquake ground motions utilized to perform the inelastic response history analyses comprise primarily the three components of the near field natural records registered at the aforementioned stations AQA, AQG, AQK and AQV during the 2009 L'Aquila earthquake. Two structural models were considered in the parametric study: a sample RC cantilever column and a two-storey two-bay frame, designed for gravity loads only (non-ductile frame).

Results of extensive parametric inelastic dynamic analyses carried out on the sample structural systems show that the variation of axial loads is significant in columns under HVGMs, especially in compression. For values of normalized axial loads (ν) corresponding to actual RC columns in building farmed structures, e.g., normalized axial load $\nu>0.10$, the average increase in the compression load ranges between ~175% ($\nu=0.20$) and ~60% ($\nu=0.50$). For high values of normalized axial loads, e.g. $\nu>0.30$, the computed axial load-bending moment interaction points lie beyond the threshold interaction curves thus indicating that failure will occur. Conversely, for normalized axial loads $\nu\leq0.20$, large fluctuations of moments were computed. Finally, the shear demand-to-supply ratio is significantly affected by the high fluctuations of axial loads in the columns. In multi-storey framed buildings, the response of central columns is adversely influenced by the HVGMs. Shear forces are influenced by the VGMs; such influence is a function of the preload present in the columns. Differences may arise particularly for low values of the normalized axial loads due to the occurrence of cracking. Shear demand is higher for lower values of normalized axial loads, e.g. $\nu<0.10$. The stiffness degradation and the strength deterioration of the RC members is lowered as the axial loads increase, Moreover, columns with higher axial loads displace less laterally and hence the base seismic shear demand is lowered.

The above discussion demonstrates that, for a given level of axial loads, the effects of the VGMs on RC beam-columns are two-fold. The shear demand is increased and the supply is

reduced due to the large variation of the axial forces. It is thus concluded that the reliable seismic design and assessment of RC framed structures should encompass both horizontal and vertical earthquake ground motions, especially for sites close to active fault, such as the case of L'Aquila studied above.

REFERENCES

Alaghebandian, R., Shiohara, H. and Otani, S. (1998). Non-linear Response of RC Framed Buildings Subjected to Horizontal and Vertical Seismic Motion, Annual Meeting of AIJ, Kyushu, Japan, 11-12.

Alaghebandian, R., Shiohara, H. and Otani, S. (1999). Effect of Distributed Mass on Non-Linear Response of RC, Annual Meeting of AIJ, Hiroshima, Japan, 11-12.

Bozorgnia, Y. and Campbell, K.W. (2004). The Vertical-to-Horizontal Response Spectral Ratio and Tentative Procedures for Developing Simplified V/H and Vertical Design Spectra, *Journal of Earthquake Engineering*, 8(2), 175-207.

Broderick, B.M., Elnashai, A.S., Ambraseys, N.N., Barr, J.M., Goodfellow, R.G. and Higazy, E.M. (1994). The Northridge (California) Earthquake of 17 January 1994: Observations, Strong Motion and Correlative Response Analysis. Engineering Seismology and Earthquake Engineering, Research Report No. ESEE 94/4, Imperial College, London.

Button, M.R., Cronin, C.J. and Mayes, R.L. (2002). Effect of vertical motions on the seismic response of highways bridges. *Journal of Structural Engineering*, 128(12), 1551-1564.

CEN (Comité Européen de Normalisation) (2006-a). Eurocode 2. Design provisions for earthquake resistance of structures. Part 1.1: General rules and rules for buildings, CEN, Brussels, Belgium.

CEN (Comité Européen de Normalisation) (2006-b). Eurocode 8. Design provisions for earthquake resistance of structures. Part 1.3: General rules. Specific rules for various materials and elements. CEN, Brussels, Belgium.

Chioccarelli. E., De Luca, F. and Iervolino, I: (2009). Preliminary study of L'Aquila earthquake ground motion records, v.5.20, available at ***http//:www.reluis.it***.

Como, M., De Stefano, M. and Ramasco, R. (2003). Effects of column axial force-bending moment interaction on inelastic response of steel frames. *Earthquake Engineering and Structural Dynamics*, 32(12), 1833–1852.

Elgamal, A. and He, L. (2004). Vertical earthquake ground motion records: An overview. *Journal of Earthquake Engineering*, 8(5), 663–697.

Elnashai, A.S., Bommer, J.J., Baron, I., Salama, A.I. and Lee, D. (1995). Selected Engineering Seismology and Structural Engineering Studies of the Hyogo-ken Nanbu (Kobe, Japan) Earthquake of 17 January 1995. Engineering Seismology and Earthquake Engineering, Report No. ESEE/95-2, Imperial College, London.

Elnashai, A.S., Papanikolaou, V., and Lee, D., (2004). "Zeus NL – A System for Inelastic Analysis of Structures", Mid-America Earthquake Center, University of Illinois at Urbana-Champaign, CD-Release 04-01.

Elnashai, A.S. and Papazoglou, A.J. (1997). Procedure and Spectra for Analysis of RC Structures Subjected to Strong Vertical Earthquake Loads, *Journal of Earthquake Engineering*, 1(1), 121–155.

Federal Emergency Management Agency (2000). State of Art Report on past performance of steel moment frame buildings in earthquakes. *Report No. FEMA 355E*. Washington, D.C., USA.

Federation Internationale Du Beton (2003). Seismic assessment and retrofit of reinforced concrete buildings. State-of-Art Report, Bulletin FIB no.24, Thomas Telford, London, UK.

Gallipoli, M.R., Mucciarelli, M. and Vona, M. (2009). Empirical estimate of fundamental frequencies and damping for Italian buildings. *Earthquake Engineering and Structural Dynamics*, 38(8), 973-988.

Goltz, J.D. (1994). The Northridge, California Earthquake of January 17, 1994: General Reconnaissance Report. National Centre for Earthquake Engineering Research, Report No. NCEER-94-0005, Buffalo.

Kim, S.J. and Elnashai, A.S. (2008). Seismic Assessment of RC Structures considering Vertical Ground Motion. MAE Center Report No.08-03, University of Illinois at Urbana-Champaign, USA.

Kunnath, S., Abrahamson, N., Chai, Y.H., Erduran, E. and Yilmaz, Z. (2008). Development of Guidelined For Incorporation of Vertical Ground Motion Effects in Seismic Design of Highway Bridges, Technical Report CA/UCD-SESM-08-01, University of California at Davis.

Kunnath, S., Abrahamson, N., Chai, Y.H., Zong, Z. and Yilmaz, Z. (2005). Effects of Vertical Ground Motions on Seismic Response of Highway Bridges, Proceedings of the Bridge Research Conference 2005, Sacramento, U.S.A., Paper No. 02-504 (CD-ROM).

MacRae, G.A., Hyde, K., Walpole, W., Moss, P., Hyland, C., Clifton, G.C. and Mago, N. (2006). Column Axial Shortening Effects in Stell Frames. *Proceedings of the 2006 NZSEE Conference*, Napier, New Zealand, CD-ROM.

Madas, P.J. and Elnashai, A.S. (1992) A new passive confinement model for transient analysis of reinforced concrete structures. *Earthquake Engineering and Structural Dynamics*, 21(5), 409-431.

Mander, J.B., Priestley, M.J.N. and Park, R. (1988). Theoretical stress-strain model for confined concrete. *Journal of Structural Engineering*, ASCE, 114(8), 1804-1826.

Martinez-Rueda, J.E. and Elnashai, A.S. (1997). Confined concrete model under cyclic load. *Journal of Materials and Structures*, 30(4), 139-147.

Masi, A. and Vona, M. (2009). Experimental and numerical evaluation of the fundamental period of undamaged and damaged RC framed buildings. *Bulletin of Earthquake Engineering (in press)*

Ministero delle Infrastrutture (2008). Decreto Ministeriale (D.M.) 14/01/2008. Technical Standards for the Constructions, Rome (in *Italian*).

Mwafy, A. and Elnashai, A.S. (2006). Vulnerability of code-compliant RC buildings under multi-axial earthquake loading. Proceedings of the 4th International Conference on Earthquake Engineering, Taipei, Taiwan (CD-ROM).

Naeim, F., Lew, M., Huang, C.H., Lam, H.K. and Carpenter, L.D. (2000). The performance of tall buildings during the 21 September 1999 Chi-Chi earthquake Taiwan. *The Structural Design of Tall Buildings*, 9(2), 137-160.

Newmark, N. M. and Hall, W. J. (1982). Earthquake Spectra and Design, EERI Monograph Series, EERI, Oakland, California.

Pacor, F. and Paolucci, R. (2009). Caratteristiche geologiche e classificazione di sito delle stazioni accelerometriche della RAN ubicate a L'Aquila. Progetto S4: BANCA DATI ACCELEROMETRICA, available at *http://esse4.mi.ingv.it (in Italian)*

Papazoglou, A.J. and Elnashai, A.S. (1996). Analytical and Field Evidence of the Damaging Effect of Vertical Earthquake Ground Motion, *Earthquake Engineering and Structural Dynamics*, 25(10), 1109–1137.

Paulay, T. and Priestley, M.J.N. (1992). Seismic Design of Reinforced Concrete and Masonry Buildings. Wiley & Sons, New York, USA.

Penelis, G.G. and Kappos, A.J. (1997). Earthquake Resistant Concrete Structures. E & FN SPON-Chapman & Hall, London, UK.

Ranzo, G., Petrangeli, M. and Pinto, P.E. (1999). Vertical Oscillations due to Axial-Bending Coupling during Seismic Response of RC Bridge Piers, *Earthquake Engineering and Structural Dynamics*, 28(12), 1685–1704.

Somerville, P. (2000). Seismic hazard evaluation. *Proceedings of the 12th World Conference on Earthquake Engineering*, Paper no.2833, New Zealand Society for Earthquake Engineering, Aukland, New Zealand, 325-346.

Watanabe, E., Sugiura, K., Nagata, K. and Kitane, Y. (1998). Performances and damages to steel structures during 1995 Hyogoken-Nanbu earthquake. *Engineering Structures*, 20(4-6), 282-290.

Youssef, N.F.G., Bonowitz, D. and Gross, J.L. (1995). A survey of steel moment-resisting frame buildings affected by the 1994 Northridge earthquake. *Report No. NISTR 56254*, National Institute for Science and Technology, Gaithersburg, Maryland, USA.